CORROSION STUDIES IN FUMING NITRIC ACID

EDSON H. PHELPS

FREDRICK S. LEE, 1ST LT.

RAYMOND B. ROBINSON

MATERIALS LABORATORY

OCTOBER 1955

PROJECT No. 7312

TASK No. 73122

WRIGHT AIR DEVELOPMENT CENTER

AIR RESEARCH AND DEVELOPMENT COMMAND

UNITED STATES AIR FORCE

WRIGHT-PATTERSON AIR FORCE BASE, OHIO

FOREWORD

This report was prepared by the Protective Processes Branch and was initiated under Project No. 7312, "Finishes and Materials Preservation", Task No. 73122. "Corrosion and Corrosion Prevention", formerly RDO 611-13, "Corrosion and Corrosion Prevention" and was administered under the direction of the Materials Laboratory, Directorate of Research, Wright Air Development Center, with Mr. E. H. Phelps as Senior Project Engineer.

This report covers work conducted from June 1953 to April 1954.
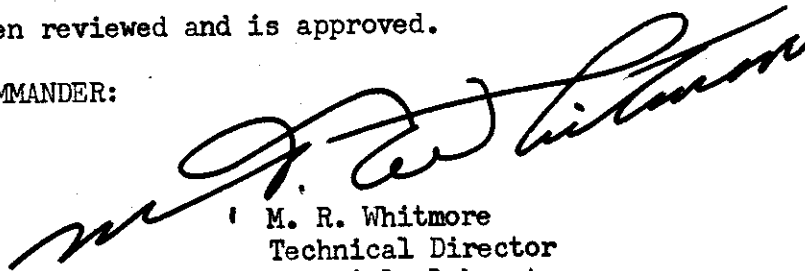
WADC TR 55-109

ABSTRACT

Tests were conducted to determine the corrosion behavior of Armco 17-7PH stainless steel alloy in red fuming nitric acid containing various amounts of hydrofluoric acid as an inhibitor. It was found that hydrofluoric acid additions to red fuming nitric acid markedly reduced the corrosion rate of the alloy. Inhibition was obtained in both liquid and vapor phases at 120°F and 160°F, for periods up to 42 days duration. It was found that a hydrofluoric acid concentration of 0.25% by weight was marginal for good inhibition, and there was some indication that a hydrofluoric acid concentration of 0.75% was optimum. The presence of glass in the system diminishes the inhibiting effect of the hydrofluoric acid.

The corrosion potential of aluminum and stainless steel electrodes was observed in fuming nitric acids with various nitrogen dioxide and water contents, and with added fluoride. It was found that water additions shift the potential of both aluminum and stainless steel in the anodic direction. Nitrogen dioxide content up to 30% did not produce a significant change in the potential of either electrode. Fluoride additions caused a definite anodic shift in the stainless steel potential, and had a tendency to shift the aluminum potential in the cathodic direction. The observed effects were correlated in a qualitative manner with the previously reported corrosion rate effects of the variables tested.

PUBLICATION REVIEW

This report has been reviewed and is approved.

FOR THE COMMANDER:

M. R. Whitmore
Technical Director
Materials Laboratory
Directorate of Research

TABLE OF CONTENTS

LIST OF ILLUSTRATIONS

INTRODUCTION

Fuming nitric acid is a highly corrosive liquid which attacks most structural metals readily. The use of fuming nitric acid as an oxidizer in liquid rocket engines has necessitated a considerable amount of research on the corrosion behavior of various metals in the acid, and on methods of preventing the corrosion obtained.

This report covers two portions of the Materials Laboratory program on fuming nitric acid corrosion. Section I covers an investigation of hydrofluoric acid as a corrosion inhibitor on Armco 17-7PH stainless steel. This investigation was prompted by previous studies which established hydrofluoric acid as a very promising corrosion inhibitor for both aluminum and austenitic type stainless steels in fuming nitric acid. The Armco 17-7PH alloy was used because of its desirable high strength properties. Section 2 covers an investigation of the solution or corrosion potential of stainless steel and aluminum in fuming nitric acid. The purpose of these studies was to determine any possible correlation between the observed potential and the previously reported corrosion rate behavior of these metals under conditions of varying nitrogen dioxide and water contents, and with added fluoride.

SECTION I

Hydrofluoric Acid as a Corrosion Inhibitor

Armco 17-7PH Stainless Steel in Red Fuming Nitric Acid (RFNA)

A. INTRODUCTION:

The purpose of this work was to determine the inhibiting effect of hydrofluoric acid additions on the corrosion rate of 17-7PH stainless steel in red fuming nitric acid containing 12% nitrogen dioxide.

Corrosion tests with uninhibited and inhibited RFNA were conducted in closed, Teflon lined pressure bombs at 120°F. The effect of added HF was evaluated primarily on the basis of weight loss versus time curves. The corrosion weight loss data were supplemented by microscopic examination of the corroded specimens. The results presented are based on the initial HF concentration in the acid, since difficulties were encountered in accurately determining the HF content after the corrosion test periods.

This report covers results obtained on hardened 17-7PH stainless steel, an alloy of interest because of its high strength characteristics.

This investigation was prompted by previous studies (1,2)* which indicated that hydrofluoric acid (HF) additions markedly reduced the corrosion rates of both austenitic type stainless steel alloys and aluminum alloys.

B. EXPERIMENTAL PROCEDURES:

1. Specimen Preparation: The 17-7PH stainless steel used in the corrosion tests was obtained from the Armco Steel Corporation, Middletown, Ohio. The metal was received as .042" X 12" X 12" samples in the annealed condition. The analysis of the material, as reported by Armco, is given in Table I. Sections 6" X 6" were cut from the samples and given the following two stage heat treatment:

(1) Held at 1400°F for 90 minutes - Air cooled at 200°F, Water quenched to 60°F.

(2) Held at 1070°F for 90 minutes - Air cooled.

The properties obtained with this heat treatment are given in Table 2. After heat treatment the sections were sand blasted to remove scale, and sheared into specimens 1cm X 3cm. Holes were punched in the specimens for mounting and identification marks stencilled into the lower edges. The specimens were then degreased with menthanol, washed with soap and water,

* Numbers in parentheses refer to listings in the Bibliography.

TABLE I

Analysis of Armco 17-7PH Stainless Steel Used in Corrosion Tests

C	–	0.073%
Mn	–	0.68
P	–	0.025
S	–	0.015
Si	–	0.47
Cr	–	16.99
Ni	–	7.20
Mo	–	0.09
Cu	–	0.15
Al	–	1.08

TABLE 2

Physical Properties of Armco 17-7PH Stainless Steel after Heat Treatment

Yield Strength*	Tensile Strength	% Elongation	Rockwell C Hardness
161,900 psi	192,400 psi	8%	42

* All values are averages of three specimens cut from sheet subjected to same heat treatment as was given the corrosion specimens.

WADC TR 55-109

-3-

and abraded, first with 180 grit and then with 240 grit alundum paper to produce a reproducible surface. After a final water wash and degreasing operation, the specimens were weighed to the nearest one tenth (0.1) milligram. The actual surface area of the test specimens was 6.66 square Centimeters. After the corrosion tests, the specimens were rinsed with water and the corrosion products *removed with a rubber eraser*. They were then rinsed with water and menthanol and reweighed.

    2. <u>Test Media</u>: All of the corrosion tests of this section were conducted in a red fuming nitric acid containing 12% NO_2, obtained from the General Chemical Company in a 55 gallon aluminum drum. Chemical analysis of this acid according to the procedures outlined in WADC Technical Report 53-6 showed that the acid as taken from the drum contained 1.1% H_2O, 11.98% NO_2, 0.063% Al.

    Hydrofluoric acid additions were made by pipetting measured volumes of a 48% by weight solution of the HF into known volumes of the RFNA. The density of the RFNA was taken as 1.54 gms/cm^3 and the HF solution as 1.15 gms/cm^3. The HF concentration figures given in this report were calculated on the basis of grams HF/gram RFNA X 100, and are therefore weight percentage of anhydrous HF.

    3. <u>Test Containers</u>: All of the tests covered in this report were conducted in sealed stainless steel bombs with Teflon liners. Two size bombs were used. The Teflon liners were machined from bar stock. Kel-F sample holders were cut from sheet stock. Figure I shows the large and small bombs, the Teflon liners, and the Kel-F sample holders. The large size bombs permitted evaluation of both liquid and vapor phase corrosion. The liquid phase only was evaluated in the small bombs. One hundred and twenty-five cc of acid was used in the large bombs and 75cc in the small bombs. Since two specimens were exposed to the liquid phase in each case, the specimen surface to volume of test media ratio was 0.160 cm^2/cm^3 in the large bombs and 0.178 cm^2/cm^3 in the small bombs. The ullage (rate of gas volume to total volume of container) was approximately 55% in the large bombs and 43% in the small bombs.

    4. <u>Calculation of MPY Values</u>: The following formula was used to convert weight loss to corrosion rate in terms of mils per year:

$$MPY = \frac{W}{A} \times \frac{1}{D} \times \frac{1}{d_1} \times 10^3$$

Where W = weight loss of a specimen
      A = area of specimen (6.66 cm^2)
      D = time of exposure - days
      d_1= density of 17-7PH alloy = 7.69 gms/cm^3

C. <u>DISCUSSION AND RESULTS</u>:

    1. <u>Uninhibited Corrosion Tests</u>: The corrosion behavior of the 17-7PH alloy in RFNA at 120°F was determined to provide a valid base point for the

inhibition tests. Weight loss versus time curves were obtained by starting a series of bomb tests at one time, and then removing a single bomb from test at intervals for weight loss determinations. The results of this type of test at 160°F and 120°F are shown in Figure 2 and 3. Each point is the average of duplicate specimens, exposed simultaneously.

Weight loss versus time curves have the advantage of showing how the corrosion rate varies with time. The slope of the curve at any given time is the corrosion rate at that time.

High corrosion rates were obtained in both liquid and vapor phases at 160°F. The leveling off of the 160°F liquid phase curve is attributed to build-up of corrosion products in the system. Linear weight loss-time curves were obtained in both liquid and vapor phases at 120°F during the 8 day test period (Figure 3). The vapor phase weight loss apparently remains low until after an incubation period of about 1 1/2 days.

The corrosion visually observed on the specimens exposed to uninhibited RFNA at 120°F and 160°F was uniform in nature. A photomicrograph of the surface of a specimen exposed to the liquid phase for 4 days at 160°F is shown in Figure 10. The corrosion apparently proceeds in an intergranular manner. The alloy appeared to be somewhat more susceptible to attack in the cold worked areas (around stencil marks and close to the sheared edge). A thin, non adherent white film was visible on the specimens after they had been removed from the acid, washed with water, and allowed to dry.

Stress corrosion cracks occurred in the stencilled areas at 120°F, when specimens were exposed to either the liquid or vapor phase. Practically every specimen tested at 120°F in uninhibited acid was cracked to some extent. No cracks were found at 160°F, probably because the excessive corrosion obtained relieved the residual stresses in the stencil marks. A representative cracked specimen is shown in Figure 9, and a photomicrograph of the root of one of the cracks is shown in Figure 11.

2. Short Time Tests with Inhibited Acid: A series of short time (one and two day) tests were conducted at 120°F and 160°F with a range of HF concentration. The purpose of these tests was first to determine the order of magnitude of inhibition to be expected, and secondly, to determine if there was a concentration range over which inhibition would be at a maximum.

The results of these tests, along with the uninhibited corrosion rates, are given in Figures 4 and 5. It can be seen that HF very effectively inhibits the corrosion of the 17-7PH alloy at 120°F and 160°F, in both liquid and vapor phases. The use of glass sample holders nullified the inhibiting effect of the HF in the liquid phase at 160°F (Figure 4). The HF probably reacts with the glass, forming a product which is non-inhibiting.

At 160°F, Figure 4, and HF concentration of 0.25% appears to be insufficient to produce good inhibition. Progressively more inhibition was obtained in the liquid phase as the HF concentration was increased from 0.50% to 1.5%. The results at 120°F (Figure 5) give some indication that the inhibitor is most effective in the concentration range of from 0.5 to 1.0%.

At the completion of above tests, the appearance of the specimens was essentially unchanged. Examination with a binocular microscope showed a very slight etching type attack on the surfaces. Very small, colorless, crystalline deposits at scattered points were visible on some of the specimens. The specimens tested with the glass holders were covered with a heavy transparent coarse deposit. The acid media were clean in all cases, whereas even one day test with uninhibited acid at 160°F produced the typical dark discoloration.

3. <u>Longer Time Test with Inhibited Acid</u>: A group of experiments were conducted to determine the inhibiting effect of the HF over longer time periods. Based on the results of the short time tests, an HF concentration of 0.75% was used in most of the longer time tests.

Weight loss-time curves in inhibited acid at 160°F and 120°F are shown in Figure 6. The 160°F data shown were obtained with large bombs, the 120°F data with the small bombs. The W/A values for the duplicate samples compared within 5%, but some scatter between samples in different bombs is apparent; especially weight loss and time in both the liquid and vapor phase. This means that the corrosion rate in the inhibited acid decreases with increasing time of exposure. The curves shown in Figure 5 indicate that temperature does not have too much effect on the corrosion rate of the 17-7PH alloy in inhibited acid.

The 120°F data were extended to a total time of 42 days in a test in which bombs were removed after 11, 21, 32 and 42 days of test. The results are shown in Figure 7, along with the 8 day 120°F results of Figure 6 for comparison. The 10-42 day weight loss time curve was steady and corresponds to a corrosion rate of 1.7 MPY. The corrosion rate was also constant in the vapor phase and corresponded to only 0.16 MPY. It can be seen that the best curve based on the 8 day test results (dash line) does not coincide with the curve through the 10-40 day test results. This may have been due to fact that the larger bombs were used in the latter test, whereas small bombs had been used in the 8 day test. Due to difficulties encountered in the analysis of the inhibited acids, the HF concentrations at the end of the above test are not known.

Experiments in small bombs extending over 21 days were conducted with acids containing 0.25 and 1.25% HF. The results are presented in Figure 8, along with those obtained with 0.75% HF. The 11 day test result with 0.25% HF definitely indicates that this concentration is border line for producing good inhibition. The corrosion rate obtained with 1.25% HF is slightly higher than that obtained with 0.75%.

Specimens exposed for the longer periods with 0.75% HF were almost identical in appearance to those described previously for the one and two day tests. A thin, glassy, bluish film was visible over portions of the vapor phase specimens. The specimens exposed to acid containing 0.25% HF for 11 days were visibly corroded. A thin, dark green deposit was visible on the specimens exposed for 21 days to acid containing 1.25% HF.

Stress Corrosion cracks were found on only one of the specimens exposed to the inhibited acid. This specimen had been exposed to RFNA containing 0.75% HF for two days at 160°F. When this is compared to the large number of cracks obtained in the uninhibited acid tests, it is concluded that HF additions reduce the susceptibility of the alloy to stress corrosion cracking in RFNA.

D. SUMMARY:

The 17-7PH alloy corroded at a high rate in both the liquid and vapor phase when exposed to RFNA containing 12% NO_2 at 120°F and 160°F.

Powerful inhibition of the corrosion of the 17-7PH alloy in RFNA at 120°F and 160°F is obtained by the addition of HF to the acid. Inhibition is obtained in both liquid and vapor phases.

Under the conditions of the laboratory type tests conducted, the addition of 0.75% HF to RFNA reduces the 120°F corrosion rate of the 17-7PH alloy to 1.7 MPY in the liquid phase and 0.16 MPY in the vapor phase, for a period of at least 42 days.

The presence of glass in the system dimishes the inhibiting effect of the HF.

HF concentration of 0.25% is marginal for producing good inhibition. There is some indication that 0.75% HF is optimum for producing maximum inhibition.

The 17-7PH alloy is susceptible to stress corrosion cracking in RFNA containing 12% NO_2. The addition of HF to the acid reduces the susceptibility of the alloy to stress corrosion cracking.

SECTION II

Potential Measurements in Fuming Nitric Acid

A. INTRODUCTION:

The purpose of this work was to observe the corrosion potentials of aluminum alloy, 1100 (2S), and type 347 stainless steel in fuming nitric acids of various nitrogen dioxide and water contents, and with fluoride additions. It was also the purpose of this investigation to determine if there is any correlation between the observed potentials and the reported corrosion behavior of the above metals in fuming nitric acids of varying nitrogen dioxide and water contents, and with added fluoride.

Numerous investigations have been conducted on the resistance of various metals to fuming nitric (3, 4, 5, 6). Usually only the corrosion rate is determined, since the suitability of the metal for service depends on this value. A number of investigations have also included determination of the effect of specific additives or components of nitric acid on the corrosion rates of aluminum and stainless steel alloys.

With stainless steel alloys, the following effects have been reported:

a. **Effect of water:** In tests at 160°F with type 347 stainless steel, the corrosion rate decreased in a nearly linear manner from 270 mils per year (MPY) to 50 MPY as the total water content of white fuming nitric acid was increased from 2% to 6% (7).

b. **Effect of nitrogen dioxide** (NO_2): In tests at room temperature with type 347 stainless steel, a corrosion rate of approximately 16 MPY was obtained in acids containing 1% and 7% NO_2. In an acid containing 23% NO_2 the corrosion rate was 1 MPY (8).

c. **Effect of fluoride:** Numerous investigations have shown that fluoride is an exceptionally good corrosion inhibitor for stainless steels in fuming nitric acids at all temperatures tested (1, 2, 9) (see also Section I of this report).

The following effects have been reported on aluminum alloys:

a. **Effect of water:** In tests at 160°F with aluminum alloy, 3003 (3S), the corrosion rate remained low in white fuming nitric acid with total water contents up to about 6%. At water contents above 6% progressively higher corrosion rates were obtained (7).

In tests with aluminum alloy 1100 at room temperature, the corrosion rate increased in nitric acid with water content above about 10% (10).

b. <u>Effect of NO$_2$</u>: In tests at 160°F with aluminum alloy, 6061 (61S), a corrosion rate of about 20 MPY was obtained in acid containing 4% NO$_2$, and a corrosion rate of 80 MPY was obtained in acid containing 20% NO$_2$ (1).

In tests at room temperature with aluminum alloy 1100, the corrosion rate was 1 MPY in 1% NO$_2$ acid, 4 MPY in 7% NO$_2$ acid, and 7 MPY in 23% NO$_2$ acid (8).

c. <u>Effect of fluoride</u>: Investigations have shown that fluoride is a remarkably good inhibitor for aluminum alloys at all temperatures tested (1, 9).

B. <u>EXPERIMENTAL PROCEDURES</u>:

1. <u>Test Arrangement</u>: Figure 12 shows the cell arrangement used in this work. Not shown is the Leeds and Northrup Portable Potentiometer-Electrometer No. 7660 which was used for all potential measurements. The half-cell potentials of the aluminum and stainless steel electrodes were measured against a Leeds and Northrup Std. 1199-13 saturated calomel electrode in addition to the bright platinum electrode shown in the figure. The cells were placed in a water bath for temperature control.

A switching arrangement shown in Figure 13 measured the following pairs of electrodes:

> PLATINUM VS. STAINLESS STEEL
> PLATINUM VS. SATURATED CALOMEL
> STAINLESS STEEL VS. ALUMINUM
> PLATINUM VS. ALUMINUM
> ALUMINUM VS. SATURATED CALOMEL
> STAINLESS STEEL VS. SATURATED CALOMEL

An **auxiliary** standard Weston Cell was included in the switching circuit to extend the range of the potentiometer.

Since HF was used in some of the determinations, it was deemed necessary to have an all plastic system to reduce any interference by an attack of the HF on glass. In addition, the test cell was separated from the junction vessel by use of a flexible Kel-F tube, since it was felt that not enough diffusion of HF to the junction cell would occur to harm the cracked-glass junction vessel used to connect the saturated calomel electrode to the fuming nitric acid electrolyte. The cracked-glass junction vessel was filled with a 10% KNO$_3$ solution which was replenished before each run. The liquid level in the cracked-glass vessel was kept above that of the surrounding nitric acid so that any diffusion would be into the electrolyte rather than into the cracked-glass vessel thus protecting the calomel cell from the electrolyte.

Because of the difficulty in achieving reproducible values, a comparison cell was constructed parallel to the test cell. Any variation of parameters was always performed in the test cell.

The electrodes were supported in the fuming nitric acid from transparent Kel-F cell lids by means of Tygon gaskets. These gaskets were replaced before each run. The cell lids kept out moisture.

2. <u>Test Procedure</u>: The test cell and the comparison cell were filled with the fuming nitric acid purified by distillation via the junction tubes from the junction cell by siphoning action. This procedure eliminated any bubble formation in the junction tubes. In the runs made at 55°C, however, difficulty was encountered by bubble formation in the junction tubes. On one occasion, a potential was observed across the junction tubes of the order of 40 millivolts. Since both junction tubes were of the same length, a constant error may have been introduced which did not affect the trend of the observed potentials

The HF was produced in all runs but one by carefully placing Mallinckrodt's AR grade $KF.2H_2O$ into the test cell. This addition was accompanied by an exothermic reaction in the evolution of some NO_2 fumes.

Different NO_2 concentrations in the fuming nitric acid were made by adding solid N_2O_4 to the distilled, white, fuming nitric acid cooled to 0°C. The solid N_2O_4 was prepared by cooling NO_2 to the dry ice temperature. The NO_2 was approximately 99% pure as delivered from the Nitrogen Division of the Allied Chemical and Dye Corporation. No attempt was made toward further purification.

3. <u>Electrode Preparation</u>: The electrodes used consisted of aluminum alloy 1100, type 347 stainless steel, and bright platinum. The aluminum and stainless steel electrodes were conditioned in the following manner·

    a. Abraded with coarse emery followed by number "0" emery paper.
    b. Washed in water.
    c. Washed in methyl alcohol.
    d. Dried and pre-soaked in white fuming nitric acid for 7 hours.

It was found that the above pretreatment gave more consistent potential readings than any others attempted. The pre-soak in WFNA was particularly important from the standpoint of obtaining consistent readings. This treatment produced a dark film on the stainless steel electrodes. Interference colors were noted on the aluminum electrodes. The platinum electrode was washed in water and solvent prior to each experiment.

4. <u>Acid Distillation Apparatus</u>: Figure 14 shows the distillation apparatus which served mainly to remove metallic contaminants found in the fuming nitric acid coming from storage. Before distillation the acid was pretreated with a quantity of concentrated sulfuric acid. Approximately 5% by weight was added which caused a yellow green precipitate to form.

The fuming nitric acid was then decanted and placed in the distillation flask where a pressure of 25 mm. of mercury was acheived with a water aspirator. At this pressure the fuming nitric acid boiled in the region of room temperature. The dry ice condenser served in a dual capacity, viz., as a condenser and a trap which prevented the frequent replacing of pressure tubing.

C. RESULTS AND DISCUSSION:

In this investigation, potentials of the following couples were observed; type 347 stainless steel, aluminum alloy 1100, bright platinum, and saturated calomel. The convention adopted was to write the cathodic electrode to the left and the anodic electrode to the right, e. g., aluminum vs saturated calomel. In this system, if current were allowed to flow, it would flow from the aluminum electrode to the calomel electrode, and the observed potential is taken as a positive value.

The potential measurements made have been reduced to graphical form in which the observed potential is shown as a function of time. Ten typical runs are depicted in Figures 15 through 24. The analysis given at the bottom of each Figure represents the initial condition of the fuming nitric acid. These analyses may be somewhat in error because of inherent difficulties in present analysis procedures.

In the following considerations, it is assumed that the observed potential measurement arises from the half cell potential of the corroding metal and the calomel electrode with its junction potential. It is assumed that the calomel and the potassium nitrate solution – fuming nitric acid electrolyte junction potential remain constant even though it is suspected that there may be some change as the composition of the fuming nitric acid in the test cell is changed. In runs where additions to the test cell are made there is also the possibility of a junction potential across the connecting tube between the test cell and the junction cell. This is also assumed to be negligible since in every case the total concentration change due to the addition is small.

1. EFFECT OF TEMPERATURE:

Figures 15 and 16 show the effect of temperature on the observed potential of the aluminum and the stainless steel electrodes. The same fuming nitric acid was used in both runs. Change in temperature had little effect on the observed potential of stainless steel. With aluminum, the potential was steady at 21°C, while a definite anodic shift was obtained at 55°C.

Figure 17 and 18 show the effect of temperature with an acid of higher NO_2 content. Again, temperature had no significant effect on the stainless steel potential. The anodic shift of the aluminum potential at 55°C is not as pronounced as in the previous case.

An idea of the reproducibility of the data can be obtained by comparing the results on each pair of electrodes.

The anodic shift of the aluminum potential at the higher temperature may be indicative of film breakdown conditions (11). This would correlate with the higher corrosion rates obtained at elevated temperatures. The factors resulting in increased corrosion rates of stainless steels at elevated temperatures apparently do not affect the half cell potential.

2. EFFECT OF FLUORIDE ADDITIONS:

Figure 19 is a clear example of the effect of fluoride on the observed potentials of aluminum and stainless steel in fuming nitric acid of low NO_2 content. Figure 20 also shows the effect of fluoride addition, but in this case the NO_2 content was higher and the fluoride additions were made in increments of 0.2%, 0.4%, and 0.7% HF which was produced by the addition of $KF.2H_2O$ to the test cell.

Figure 21 shows an attempt to duplicate and extend the work shown in Figure 20 (15% NO_2 acid).

The measurements shown in Figure 22 indicate the results obtained when fluoride was added to an acid of very high NO_2 content (30%).

As the fluoride concentrations in the above runs were produced by the addition of pure solid potassium fluoride dihydrate ($KF.2H_2O$), a check was made to see if any anomalous results would occur if hydrofluoric acid per se were added. Figure 23 shows the results of this addition and should be compared to Figure 19. It should be noted that the electrolyte composition was not exactly the same in each case. With stainless steel, similar results were obtained, indicating that the source of the fluoride is not too important. This conclusion was reached in a previous investigation (9) which included both weight loss and potential measurements. The potential of the aluminum electrode showed little change as HF was added, while a noticeable change was observed in Figure 19. The same discrepancy in the effect of fluoride on the aluminum potential was noted in the duplicate runs shown in Figures 20 and 21, where the source of fluoride was the same.

The corrosion inhibiting effect of hydrofluoric acid additions in fuming nitric acids has been attributed to the formation of a tightly adherent film of insoluble metal fluorides on the surface of the metal (1). If this is the case, fluoride would be expected to function primarily at the anodic areas of the corroding metal surface, and should be classed as an anodic inhibitor. The normal attributes of an anodic inhibitor are increased polarization of the anodic areas, resulting in a decreased corrosion rate and a more cathodic corrosion potential for the metal (12).

A study of the effects of fluoride additions on the potential of aluminum in fuming nitric acid indicates that in some cases a definite cathodic shift was obtained, while in others fluoride had little effect. A factor which may explain the above discrepancy is the ability of aluminum to form an oxide film. With complete or heavy oxide film formation, i.e., after immersion in fuming nitric acid, aluminum would be expected to be under conditions of anodic control, and fluoride would not be expected to affect the potential further. However under conditions of incomplete oxide film formation, fluoride would be expected to produce a cathodic shift, as was obtained in some of the runs. The condition of the oxide film on the aluminum may also explain lack of reproducibility obtained with this electrode.

It has been noted that the effect of fluoride is to shift the potential of stainless steel anodically, which is inconsistent with the normally expected effect of an anodic inhibitor. However, it is possible that the insoluble fluoride film produced, limits the cathodic area to the extent that a high cathodic current density is obtained, resulting in a high degree of cathodic polarization. It is also plausible that the presence of a fluoride film would disturb the auto-catalytic cathodic reaction cycle which is obtained on nobler metals in nitric acids. (13, 15, 16). These considerations lead to the conclusion that the observed potential behavior is not necessarily inconsistent with the assumption that fluoride functions primarily at the anodic areas.

3. EFFECT OF WATER ADDITIONS:

The effect of water additions on the potential of aluminum and stainless steel in an acid containing 5% NO_2 is shown in Figure 24. It can be seen that there is a definite anodic shift of the potential of both metals with 5% or more added water. Figure 24 also indicates an anodic shift at the 3% added water level which is not as pronounced as that with 5% added water.

The more anodic potential and reduced corrosion rate obtained on stainless steel indicates that the effect of water additions on stainless steel is primarily one of polarization of local cathodes. This may be due to the fact that water represses the reaction which account for the referenced autocatalytic type cathodic reaction obtained in nitric acids. The dependence of the self-ionization of nitric acid to nitronium ions and nitric ions in nitric acid on the water content (14) may also be a factor.

The more anodic potential and the reported increase in corrosion rate of aluminum with added water lead one to believe that the effect water additions have on this electrode is one of anodic depolarization. This corresponds with the results of a previous investigation of the polarization characteristics of aluminum electrode in fuming nitric acid at 160°F. Here it was shown that aluminum was anodically polarized more easily at low and intermediate water contents (2 and 5% water) than at 9% total water content (17).

4. EFFECT OF NITROGEN DIOXIDE:

An indication of the effect of NO_2 on the potential of the electrodes at room temperature obtained is shown by comparing Figures 15, 19, 23 and 24 (runs with acids containing 1 to 5% NO_2), with Figures 17 and 20 (runs with acids containing about 15% NO_2), and with Figures 22 (run with acid containing 30% NO_2). In runs where additions were made only the comparison cells should be considered.

The results contained in the above mentioned figures indicate that over the time tested, NO_2 concentration did not affect the observed potential of either stainless steel or aluminum to a significant degree.

With respect to stainless steel, the insensitivity of the observed potential to NO_2 content may be explained if one envisions that as a result of the cathodic reaction process, a very high NO_2 content exists at the surface of the metal. Under these conditions, changes in bulk NO_2 content would not greatly change the high NO_2 region next to the electrode, and hence would not be expected to change the potential. The above considerations are partially confirmed by the results of corrosion tests on stainless steels under flowing conditions (18). As the velocity of flow is increased, a linear reduction in corrosion rate is obtained, presumably due to a progressive sweeping away of the lower oxides of nitrogen next to the surface, hence breaking the autocatalytic cathodic reaction cycle. It may be that the reduction in corrosion rate at high NO_2 content reported in reference (8) is due to an NO_2 induced passive condition (19), which was not obtained in these experiments.

The effect of NO_2 content on the aluminum electrode is not clear because reportedly the corrosion rate of aluminum increases both with NO_2 content (1), and with increased turbulence (18), and yet no significant effect on potential was noted as the NO_2 concentration was increased. More closely controlled and coincident experiments are required to establish the effect of NO_2 on aluminum corrosion in fuming nitric acid.

5. EFFECT OF AGITATION:

During the course of the above work, several experiments were conducted in the various acids to determine if agitation produced by a small magnetic stirrer had any effect on the observed potentials. It was found that the agitation produced by the stirrer used had little effect on the observed potentials.

6. REPRODUCIBILITY OF MEASUREMENTS:

In these experiments, stainless steel was found more reproducible as an electrode than aluminum. All readings on stainless steel (comparison cells) fell within 40 millivolt of 1120 millivolts. Readings on the aluminum electrodes varied from 720 to 460 millivolts, with the majority of readings falling in the 700-750 millivolts range. This variation in the aluminum half cell potential may be accounted for by the condition of the oxide film as mentioned previously.

7. RESULTS WITH THE PLATINUM ELECTRODE:

During the course of investigation of the aluminum vs calomel and stainless steel vs calomel cells, observations were made on the following cells existing in the apparatus shown in Figure 12:

> PLATINUM VS. STAINLESS STEEL
> STAINLESS STEEL VS. ALUMINUM
> PLATINUM VS. ALUMINUM
> PLATINUM VS. SATURATED CALOMEL

In all measurements it was possible to calculate the potential observed in the cell, stainless steel vs aluminum, from the aluminum vs calomel and stainless steel vs calomel couples as well as from the platinum vs aluminum and platinum vs stainless steel couples. On this evidence, a platinum electrode could be employed in work of this type instead of the saturated calomel electrode, which would eliminate the use of an aqueous-fuming nitric acid junction.

D. SUMMARY:

The addition of fluoride shifted the observed potential of type 347 stainless steel in the anodic direction. Fluoride additions tended to shift the potential of aluminum in the cathodic direction. The effect was more pronounced in the case of stainless steel.

The NO_2 concentration did not affect the observed potentials to a significant degree.

The water concentration of the fuming nitric acid electrolyte affected the observed potential of both the aluminum and stainless steel electrodes at total water concentrations from 5% to 10%. An anodic shift of potential was obtained with both electrodes.

An attempt was made to correlate in a qualitative manner, the observed effect of fluoride, NO_2 and water on the potential with the previously reported effects of these materials on the corrosion rate of stainless steel and aluminum in fuming nitric acids.

More refined techniques and coincident experiments may be able to elucidate further the effects of the various factors.

BIBLIOGRAPHY

1. Mason, D. M., Taylor, L. L. and Keller, H. F., Storability of Fuming Nitric
    Acid. Jet Propulsion Laboratory Report No. 20-72, California Institute of
    Technology, Pasadena, California, December 1953

2. Scheer, M. D. (U) Symposium on the Practical Factors Affecting the Application
    of Nitric Acid and Mixed Oxides of Nitrogen as Liquid Rocket Propellants.
    Research and Development Board Report No. FRO 200/12, The Department of
    Defense. March 1952. pp 238. (CONFIDENTIAL)

3. Materials for Rockets Using Nitric Acid. Aerojet General Corporation Tech-
    nical Memorandium No. 172. Aerojet General Corporation, Azusa, California.
    March 1951.

4. Corrosion Test Program No. 1. Bell Aircraft Company., Report No. BLR 51-106
    Bell Aircraft Corp., Buffalo, New York. August 1952.

5. Fontana, M. G., Material for Handling Fuming Nitric Acid. Part 1, 2, and 3,
    United States Air Force Technical Report 6519, United States Air Force,
    Wright Air Development Center. January 1954.

6. 6000 Pound Thrust Jet Propulsion Unit Part II – Materials. United States
    Air Force Technical Report 6519, United States Air Force, M. W. Kellogg Co.,
    Jersey City, New Jersey. March 1948.

7. Fontana, M. G., Materials for Handling Fuming Nitric Acid, Part 3. United
    States Air Force Technical Report 6519, United States Air Force, Wright
    Air Development Center. January 1954.

8. Quarterly Projects Report. United States Navel Air Rocket Test Station
    Report No. 30. United States Navy. April 1953.

9. Feiler, C. E. and Morrell, G. (U) Investigation of Effect of Fluoride on
    Corrosion of 2S-O Aluminum and 347 Stainless Steel in Fuming Nitric Acid at
    170°F. Research Memorandum E53L17b. National Advisory Committee for
    Aeronautics, Lewis Flight Propulsion Laboratory, Cleveland, Ohio. February
    1954. pp 8 (CONFIDENTIAL)

10. Binger, W. W., (U) Symposium on the Practical Factor affecting the Appli-
    cation of Nitric Acid and Mixed Oxides of Nitrogen as Liquid Rocket Propellants.
    Research and Development Board Report No. FRO 200/12, The Department of
    Defense. March 1952. pp 316 (CONFIDENTIAL)

11. Evans, U. R., _Metallic Corrosion Passivity and Protection._ 2nd Edition. Longmans, London. 1946. pp 759.

12. Mears, R. B. and Brown, R. H. _A Unified Mechanism of Passivity and Inhibition Part II._ Journal of the Electrochemical Society. Volume 97. March 1950. pp 75-82.

13. Evans, U. R. _Metallic Corrosion Passivity and Protection._ 2nd Edition. Longmans, London. 1946. pp 224.

14. Ladnayi, D. J., Miller, M. O., Karo, W. and Feiler, C. E. (U) _Some Fundamental Aspects of Nitric Acid Oxidants for Rocket Applications._ Research Memorandum E52J01. National Advisory Committee for Aeronautics, Lewis Flight Propulsion Laboratory, Cleveland, Ohio. January 1953. pp 17. (CONFIDENTIAL)

15. Ellingham, H. J. T., _Alternative Electrode Reactions, Part I. Reactions at a Platinum Cathode in Nitric Acid Solutions._ Journal of the Chemical Society, 1932. pp 1565.

16. Hedges, E. S. _The Action of Nitric Acid on Some Metals._ Journal of the Chemical Society, 1930. pp 561.

17. Fontana, M. G., _Materials for Handling Fuming Nitric Acid._ Part 3. United States Air Force Technical Report 6519, United States Air Force, Wright Air Development Center. January 1954. pp 9.

18. Fontana, M. G., _Materials for Handling Fuming Nitric Acid._ Part 4. United States Air Force Technical Report 6519, United States Air Force, Wright Air Development Center. March 1954. pp 18-20.

19. Evans, U. R., _Corrosion by Nitric Acid._ Transactions of the Faraday Society, Volume 40, 1944. pp 120.
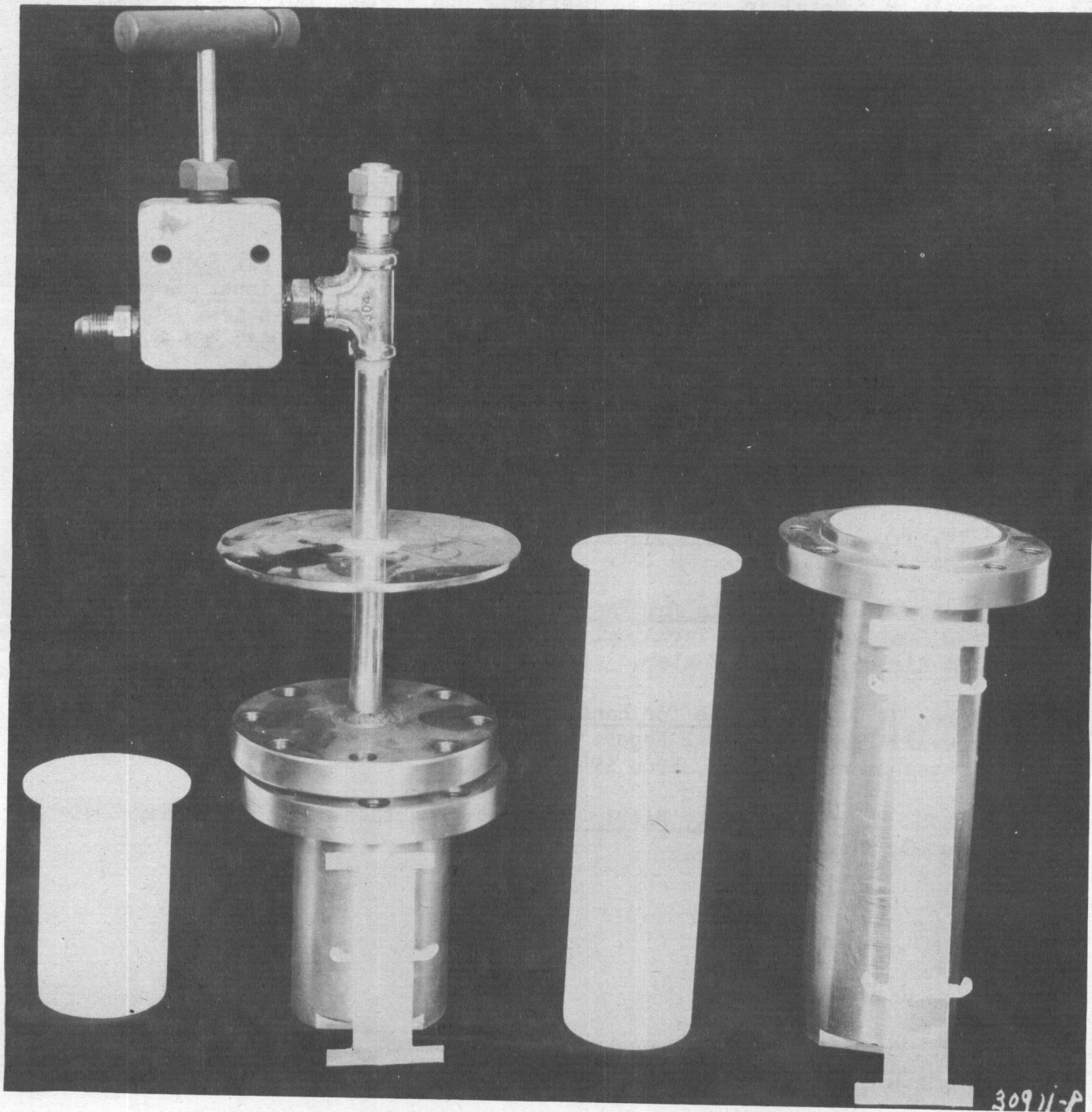
FIGURE 1   TEST APPARATUS FOR CORROSION TESTS.
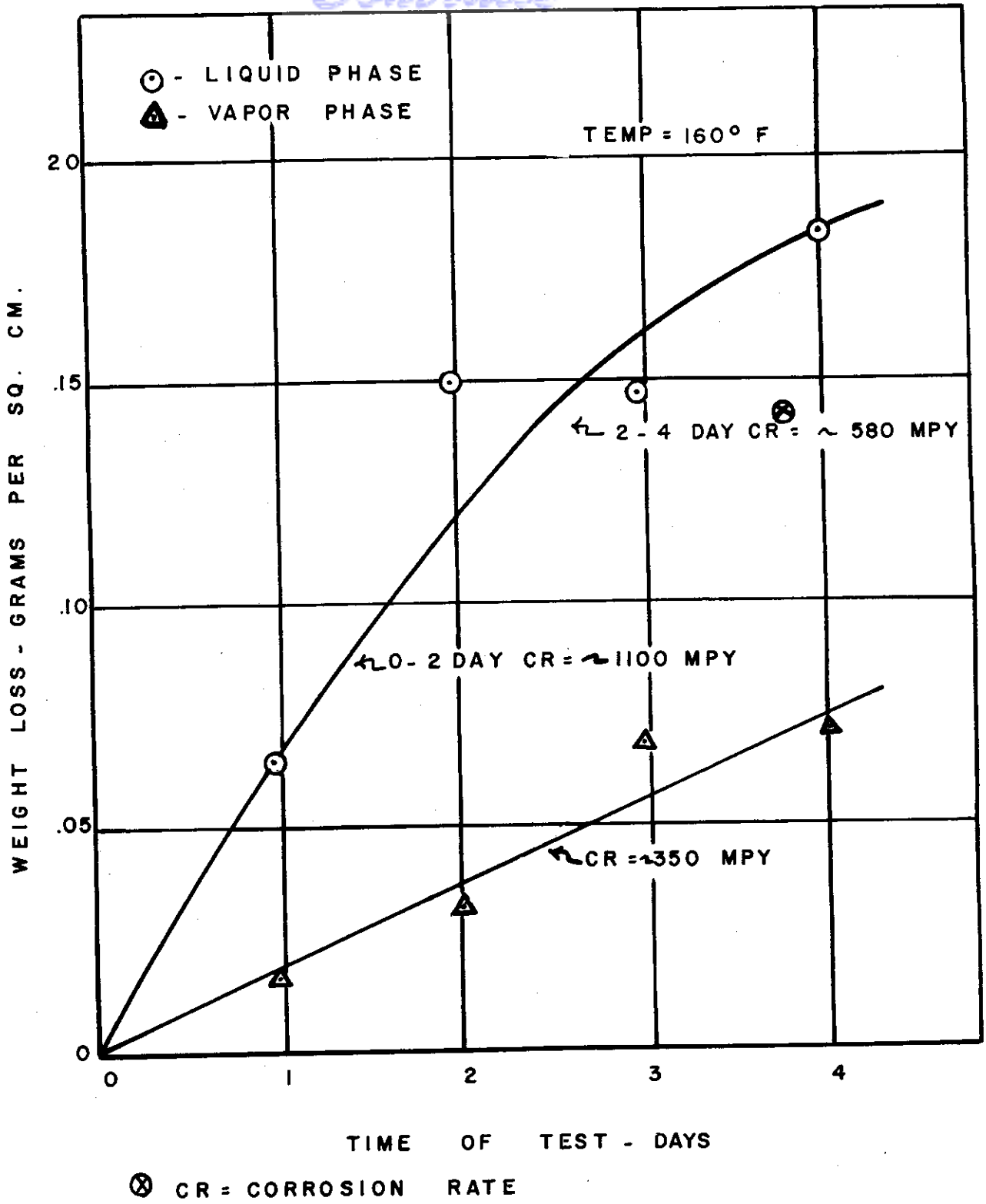
FIGURE 2 CORROSION BEHAVIOR OF ARMCO
17-7 PH SS IN UNINHIBITED RFNA (12 % NO₂)

-19-
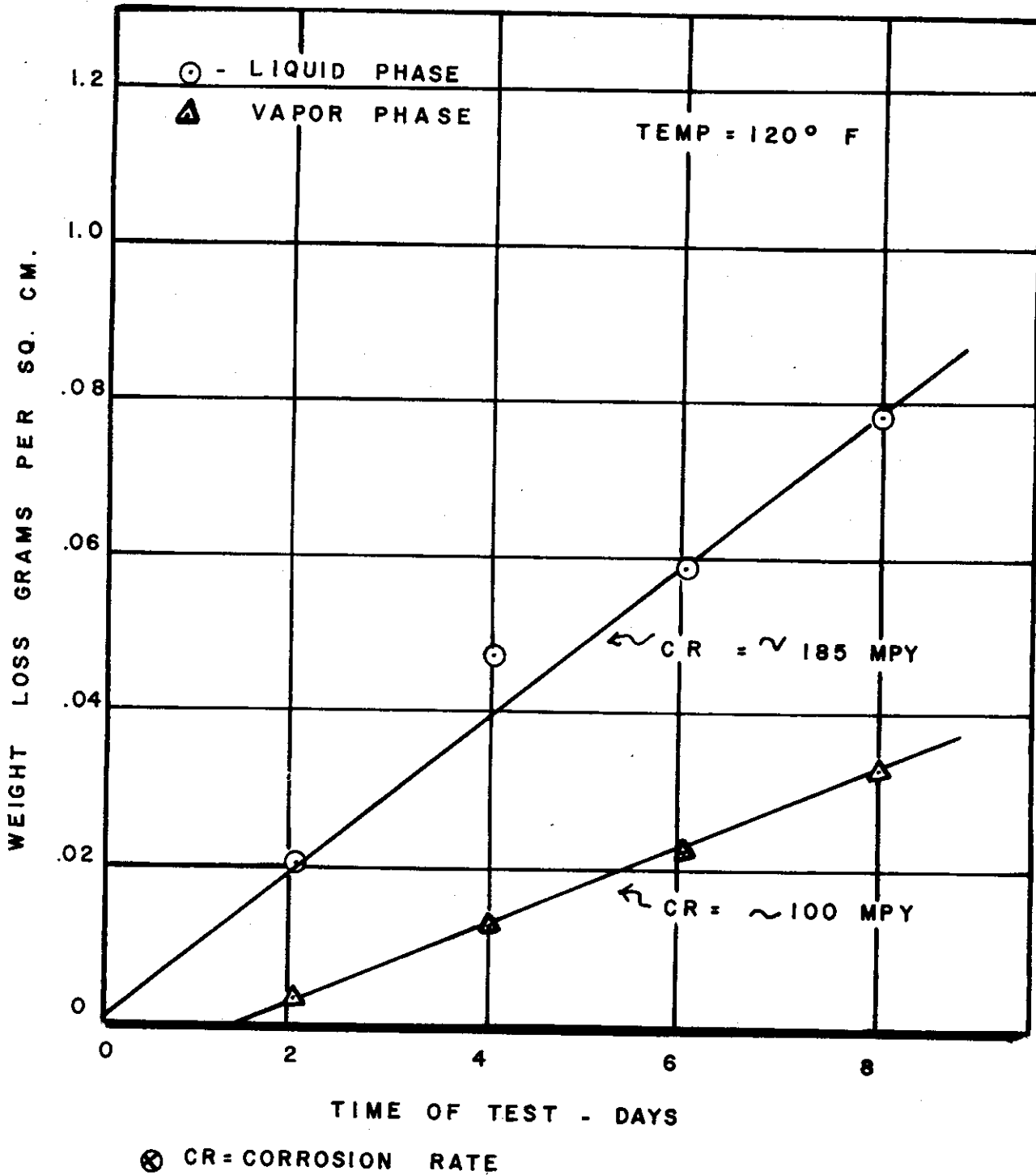
FIGURE 3 - CORROSION BEHAVIOR OF ARMCO 17-7 PH SS IN UNINHIBITED RFNA (12% NO_2)
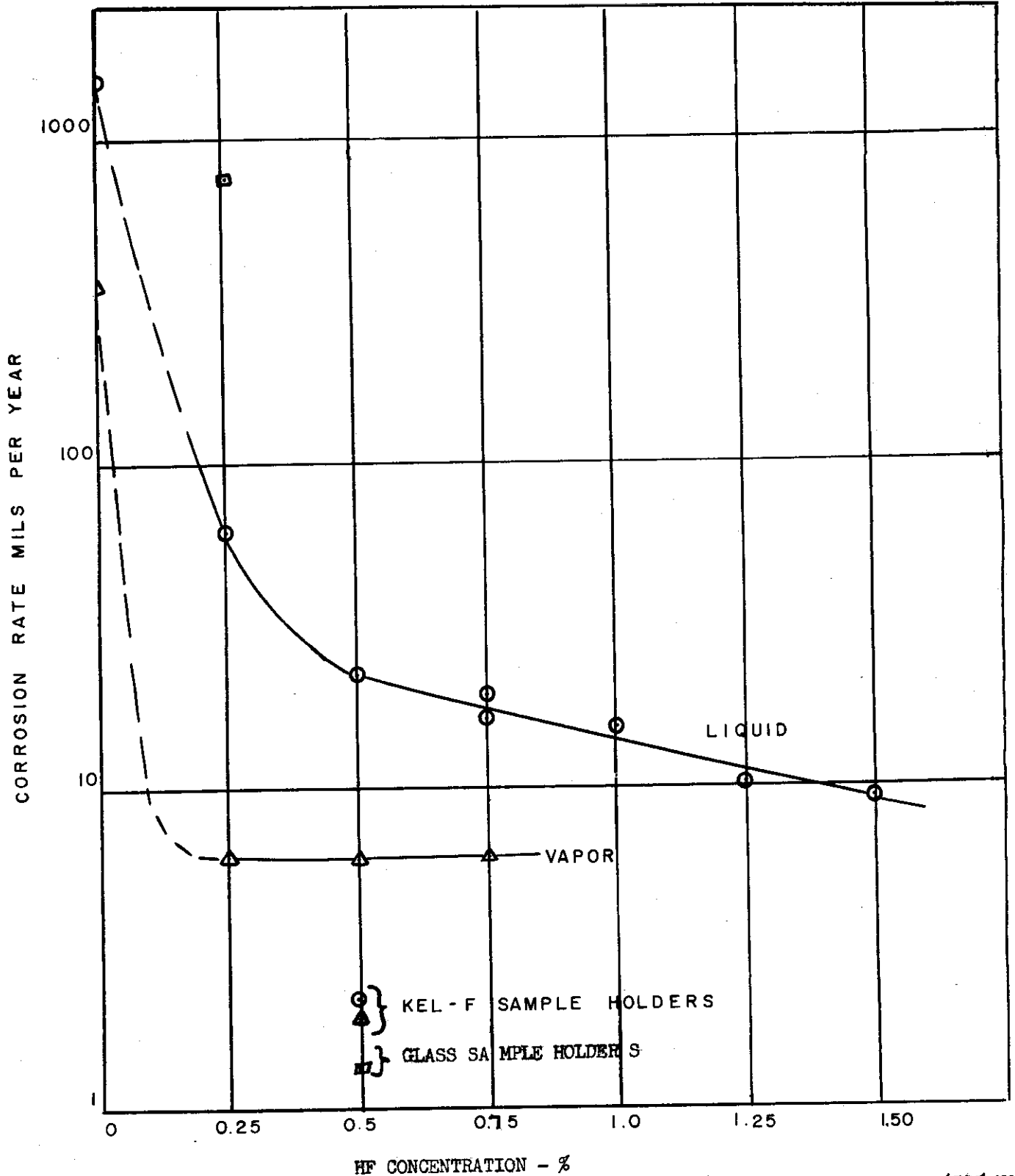
FIGURE 4 – EFFECT OF HF CONCENTRATION ON THE CORROSION OF 17–7PHSS IN RFNA (12% NO$_2$) FOR ONE DAY TESTS AT 160°F
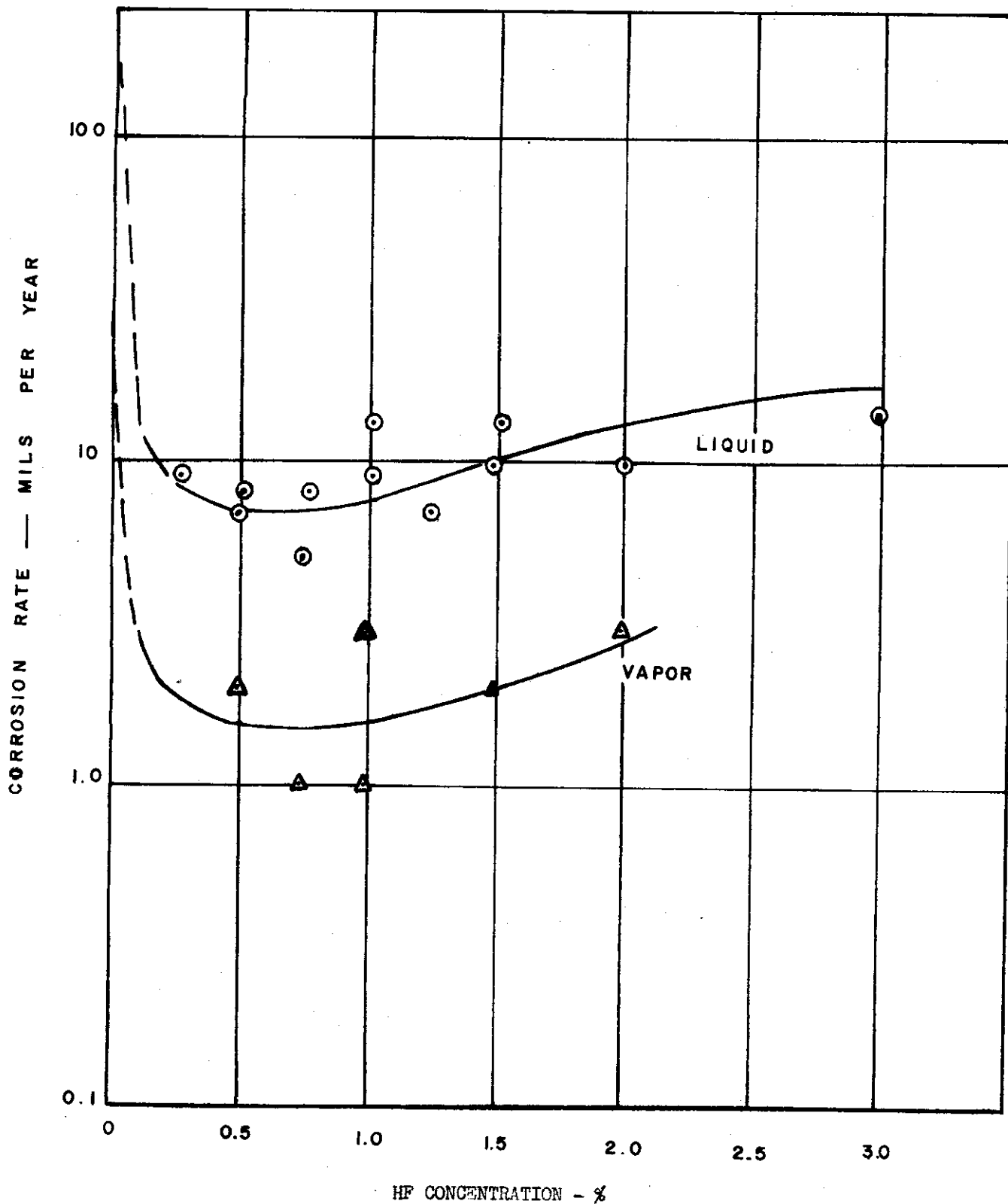
FIGURE 5 — EFFECT OF HF CONCENTRATION ON THE CORROSION OF 17-7PHSS IN RFNA (12% NO$_2$) FOR TWO DAY TESTS AT 120°F
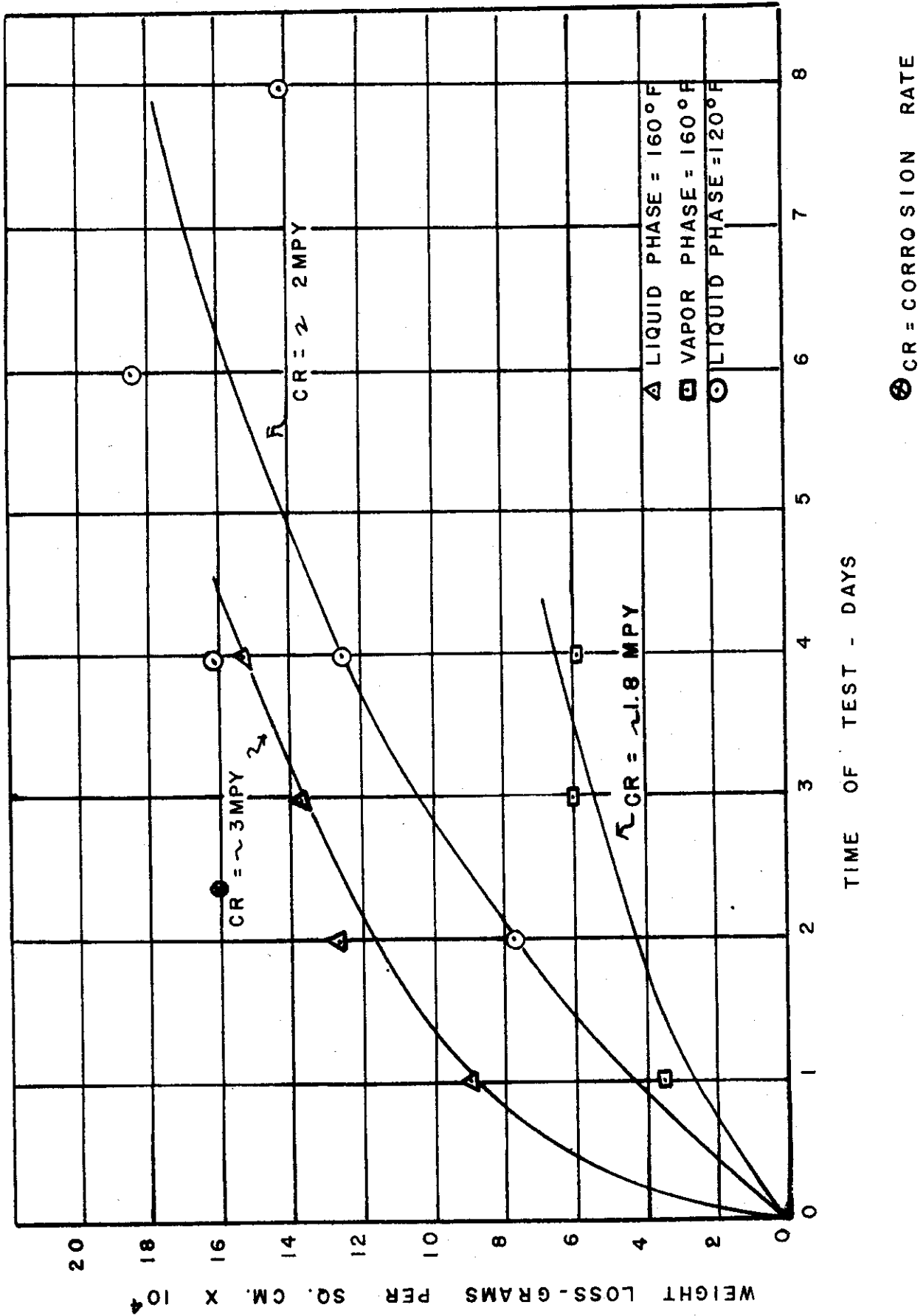
FIGURE 6 = CORROSION BEHAVIOR 17-7 PH SS
IN RFNA (12% NO$_2$) CONTAINING 0.75% HF

⊕ CR = CORROSION RATE

△ LIQUID PHASE = 160°F
☐ VAPOR PHASE = 160°F
⊙ LIQUID PHASE = 120°F

CR = ~ 3 MPY

CR = ~ 2 MPY

CR = ~1.8 MPY

TIME OF TEST - DAYS

WEIGHT LOSS-GRAMS PER SQ. CM. X 10^4
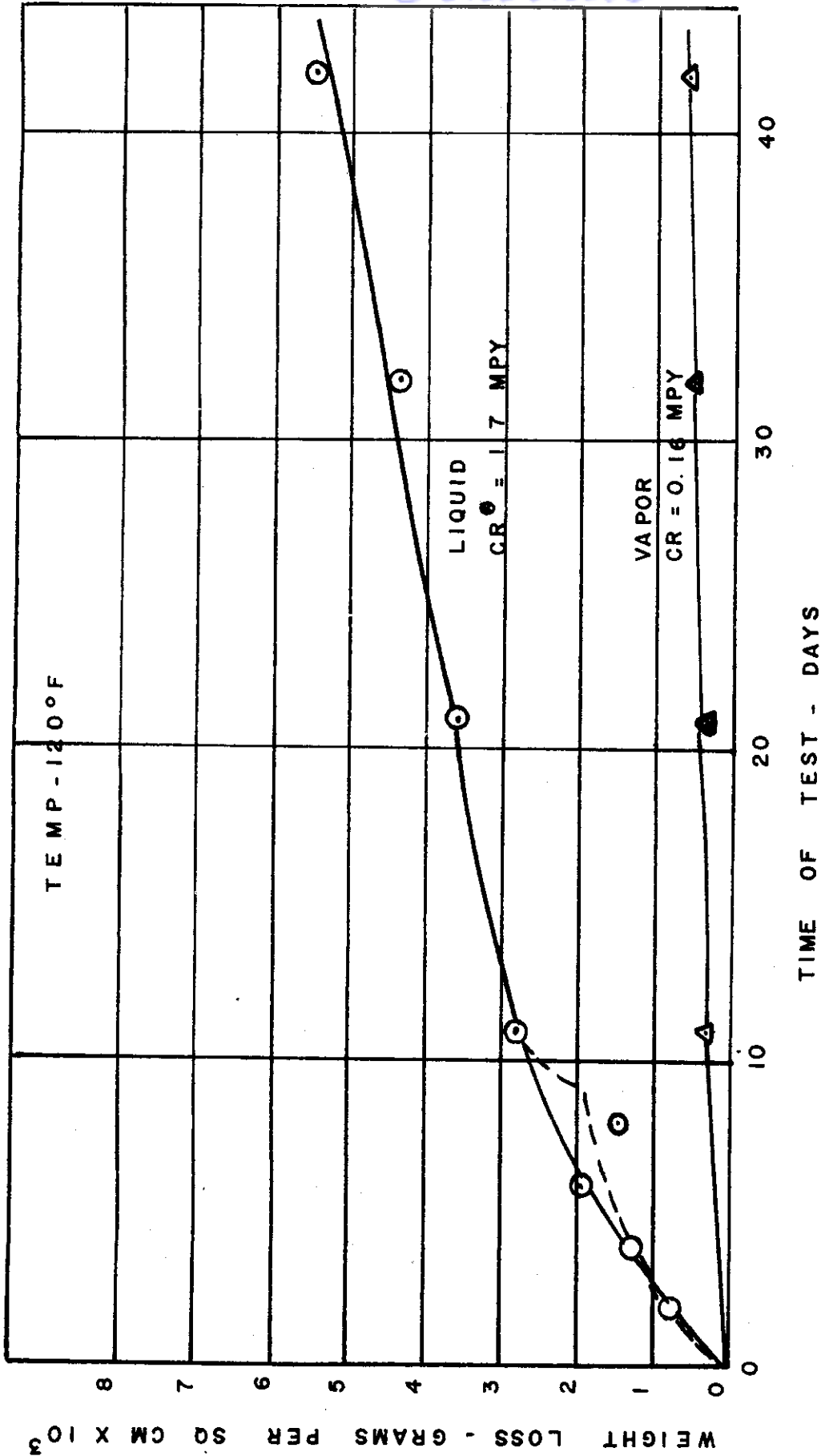
FIGURE 7 = CORROSION BEHAVIOR OF 17-7PH SS
IN RFNA(12% NO$_2$) CONTAINING 0.75% HF

TEMP-120°F

LIQUID
CR = 1.7 MPY

VAPOR
CR = 0.16 MPY

● CR = CORROSION RATE

TIME OF TEST - DAYS

WEIGHT LOSS - GRAMS PER SQ CM X 10^3
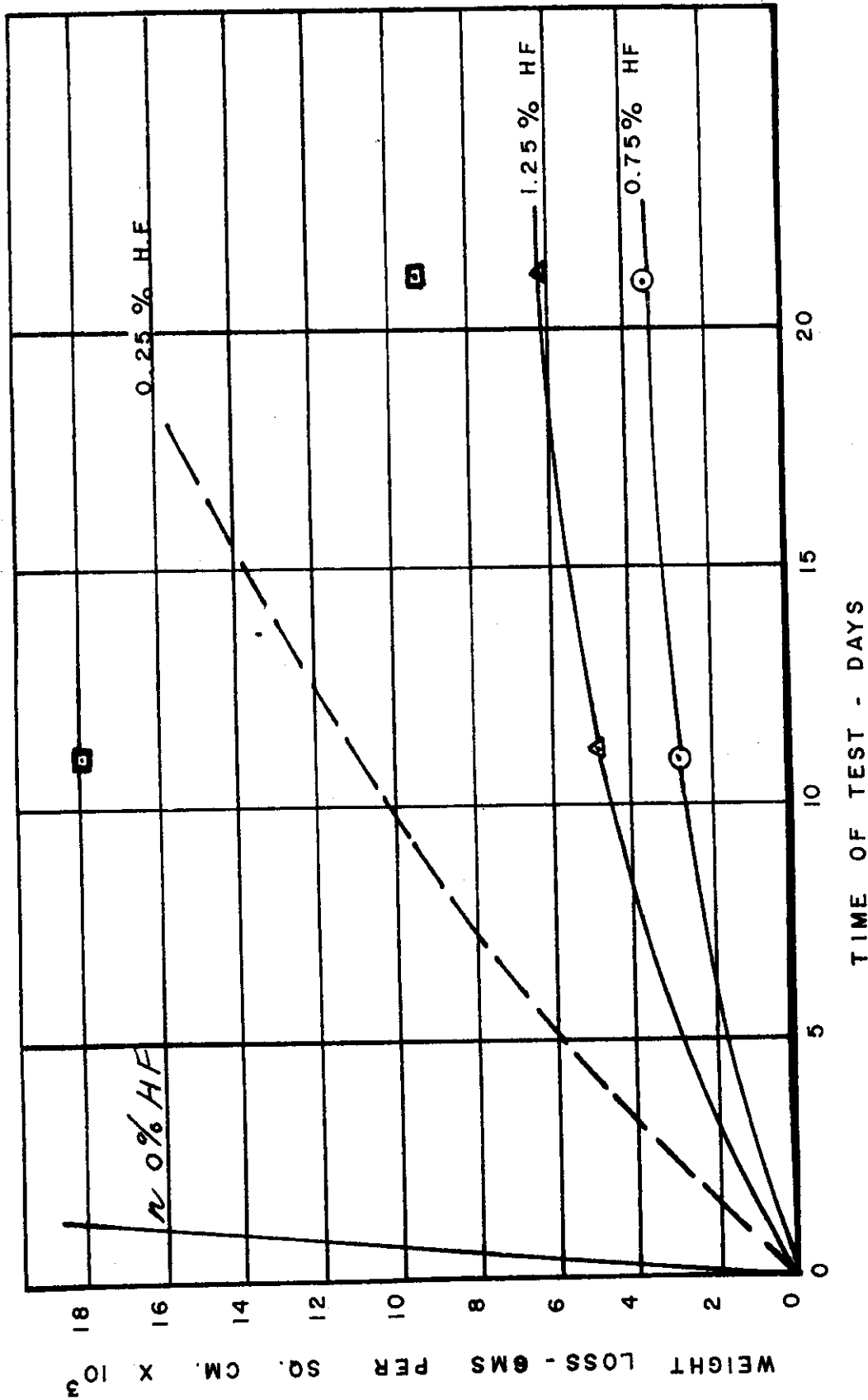
FIGURE 8 – EFFECT OF HF CONCENTRATION ON THE CORROSION OF 17-7PHSS' IN RFNA (12% NO2) FOR A 20 DAY TEST PERIOD AT 120°F
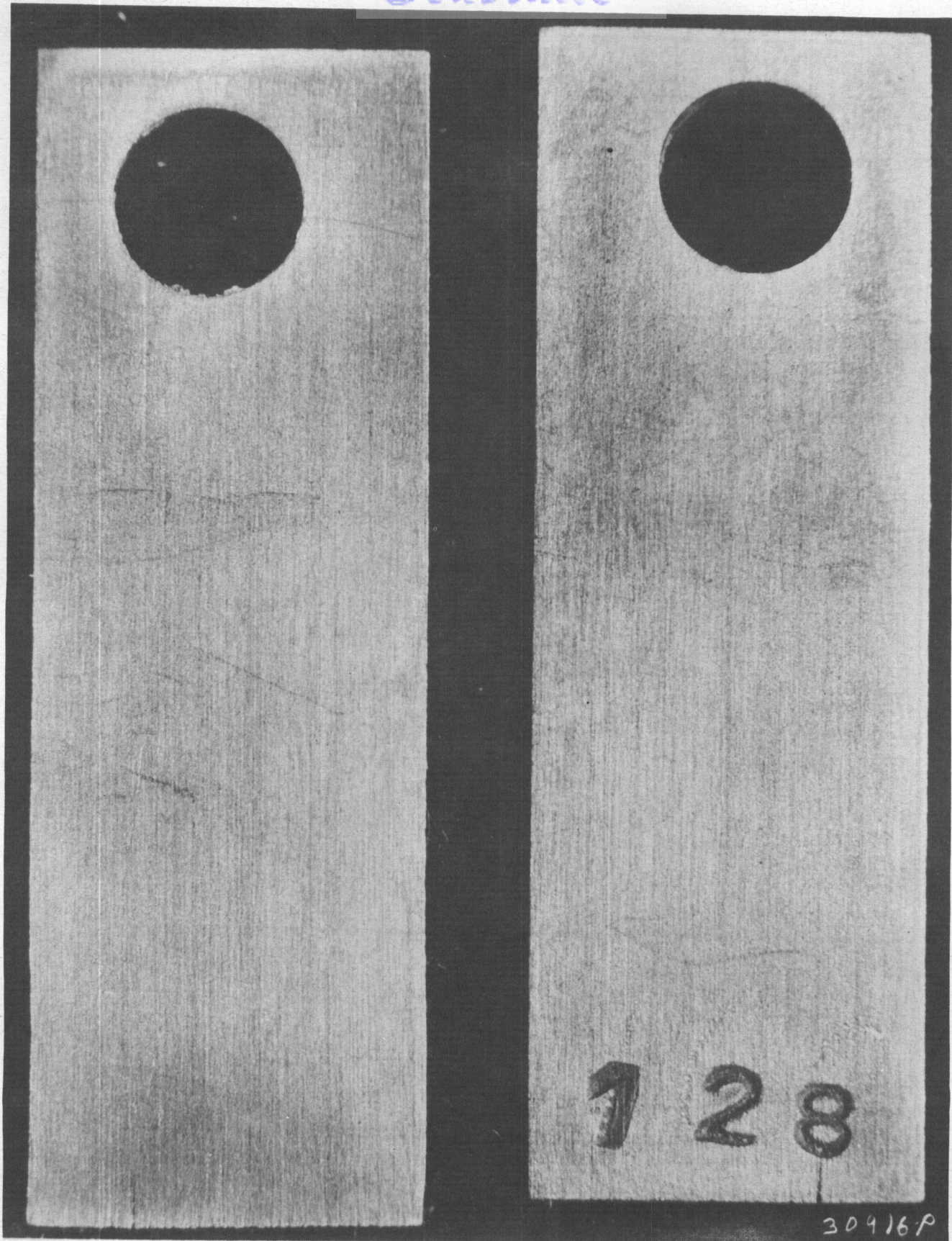
FIGURE 9 Specimen exposed to RFNA for 4 days at 120°F.
Note crack extending from stencilled number eight.
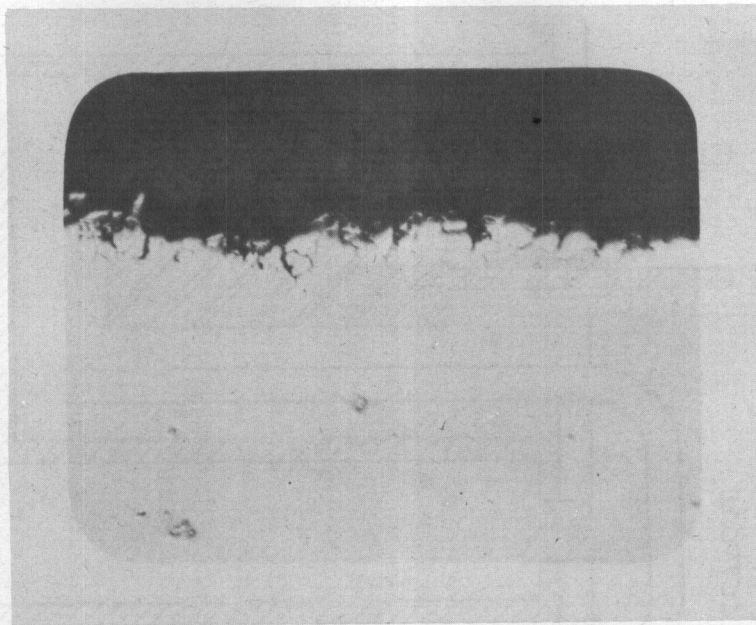
FIG __10__ PLATE __30943 M__

MAGN __X250__ DIAM ETCH __None__

REMARKS:

Surface of specimen exposed to RFNA at 160°F for 4 days
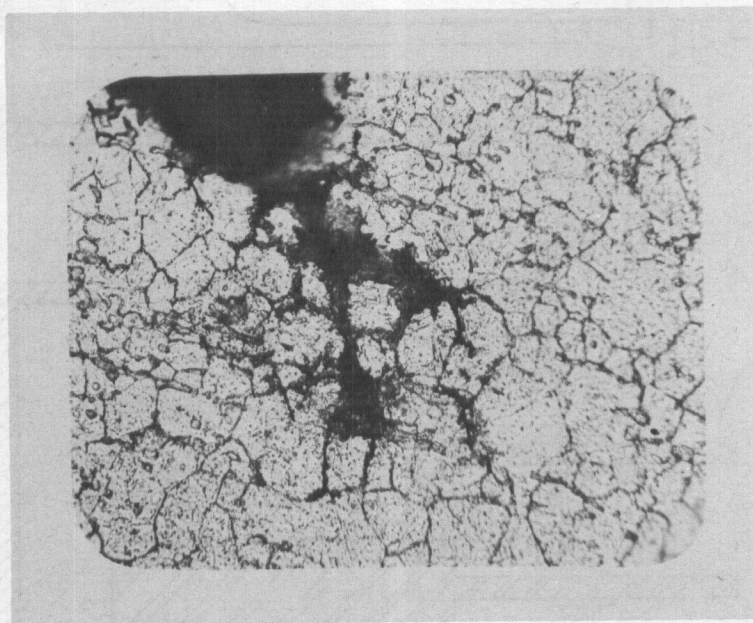
FIG __11__ PLATE __30780 M__

MAGN __X500__ DIAM ETCH __Electrolytic, 10% Chromic Acid__

REMARKS:

Root of crack on specimen exposed to RFNA at 120°F

CELLS AND JUNCTION TUBES MADE OF TEFLON

SATURATED CALOMEL ELECTRODE

BRIGHT PLATINUM ELECTRODE

TYPE 347 STAINLESS STEEL ELECTRODE

2S ALUMINUM ELECTRODE

COMPARISON CELL

JUNCTION CELL

TEST CELL
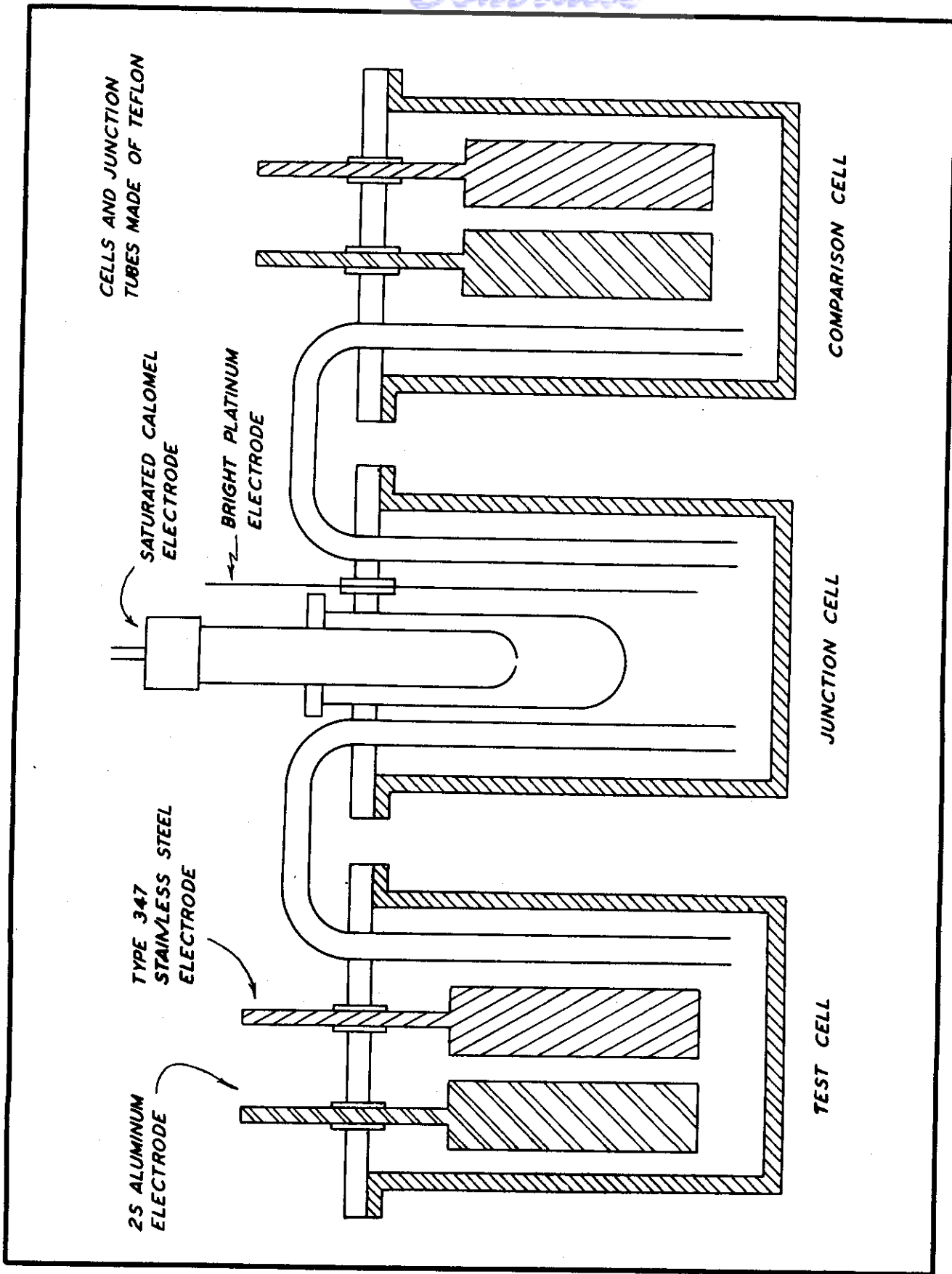
FIGURE 12 - DIAGRAM OF CELL ARRANGEMENT
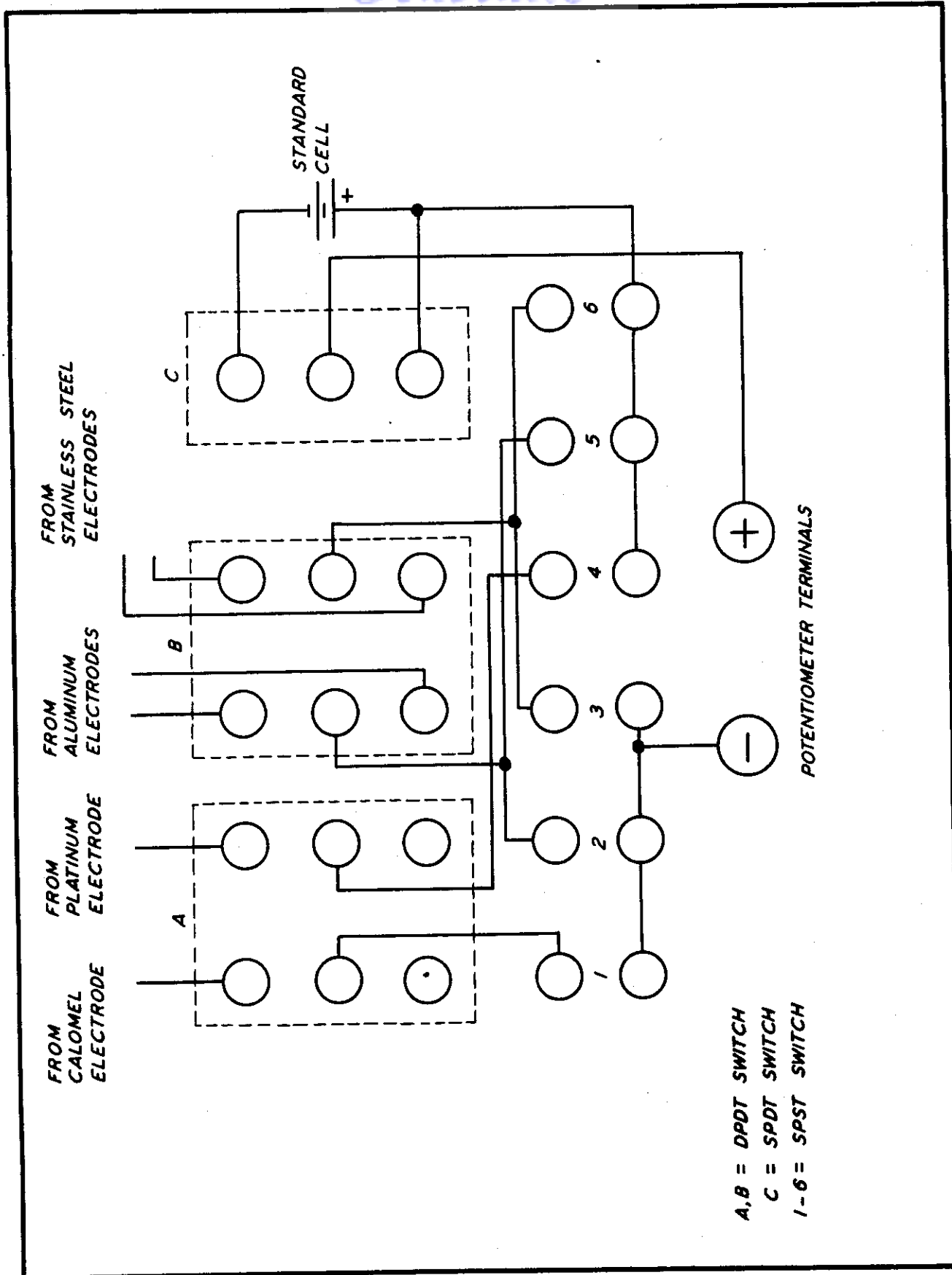
FIGURE 13 - DIAGRAM OF SWITCHING ARRANGEMENT

A,B = DPDT SWITCH
C = SPDT SWITCH
1-6 = SPST SWITCH

THERMOMETER

2 LITER 2 NECKED FLASK HEATED WITH A VARIAC CONTROLLED GLAS-COL HEATING MANTLE

TO ASPIRATOR

CAUSTIC SCRUBBER

DRY ICE CONDENSER

I LITER FLASK

TRAP

MANOMETER

VENT

JOINTS LUTED WITH FLUOROLUBE GREASE
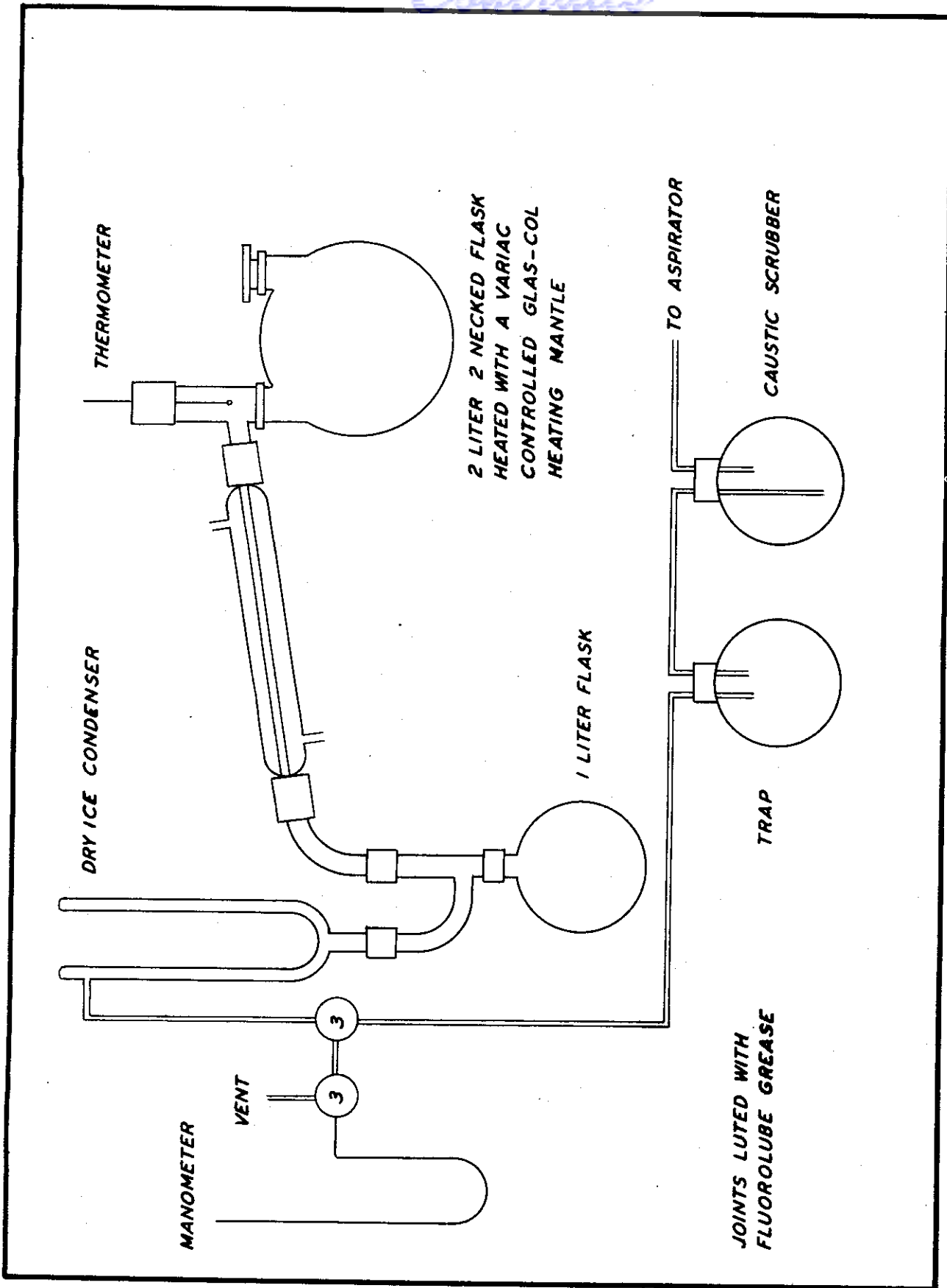
FIGURE 14 – DIAGRAM OF DISTILLATION APPARATUS

FIGURE 15 - EFFECT OF TIME ON POTENTIAL AT 21°C (4% NO₂ ACID)

GRAPH I   RUN 30, 21°C, 95.17% HNO₃ , 4.48% NO₂ , 0.34% H₂O

STAINLESS VS. CALOMEL STEEL

ALUMINUM VS. CALOMEL

REGIONS A AND B SHOW
POTENTIAL CHANGE WITH
TIME OF 2 DIFFERENT
PAIRS OF ALUMINUM
AND STAINLESS STEEL
ELECTRODES

—FIGURE 16 — EFFECT OF TIME ON POTENTIAL AT 19°C IN 12% NO_2 ACID
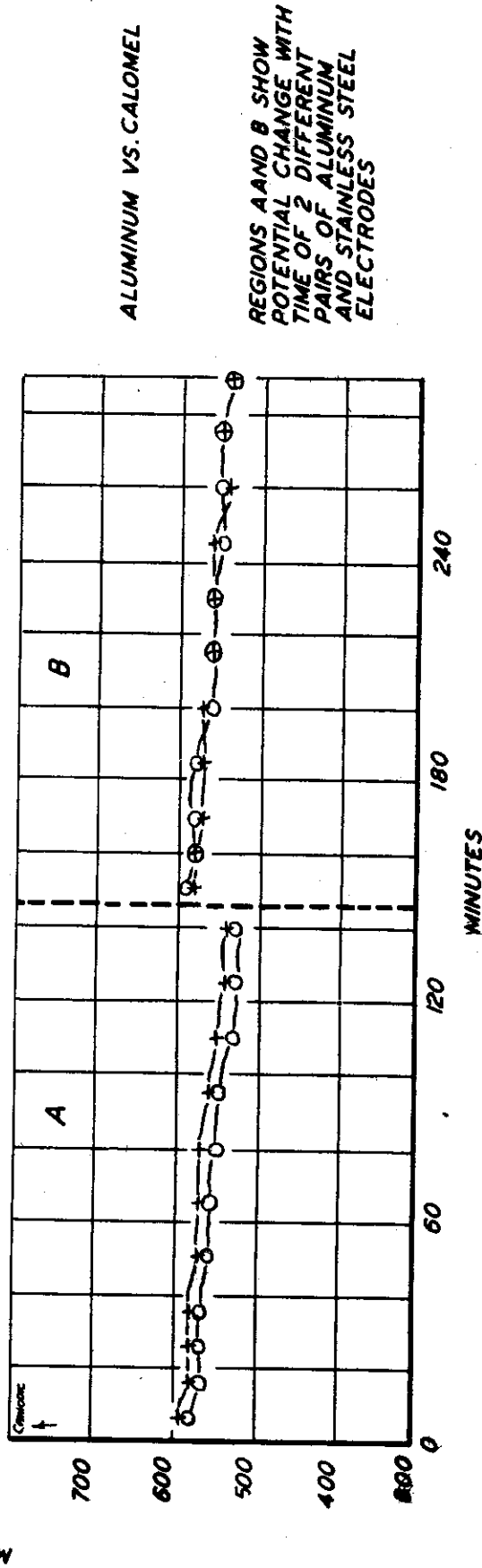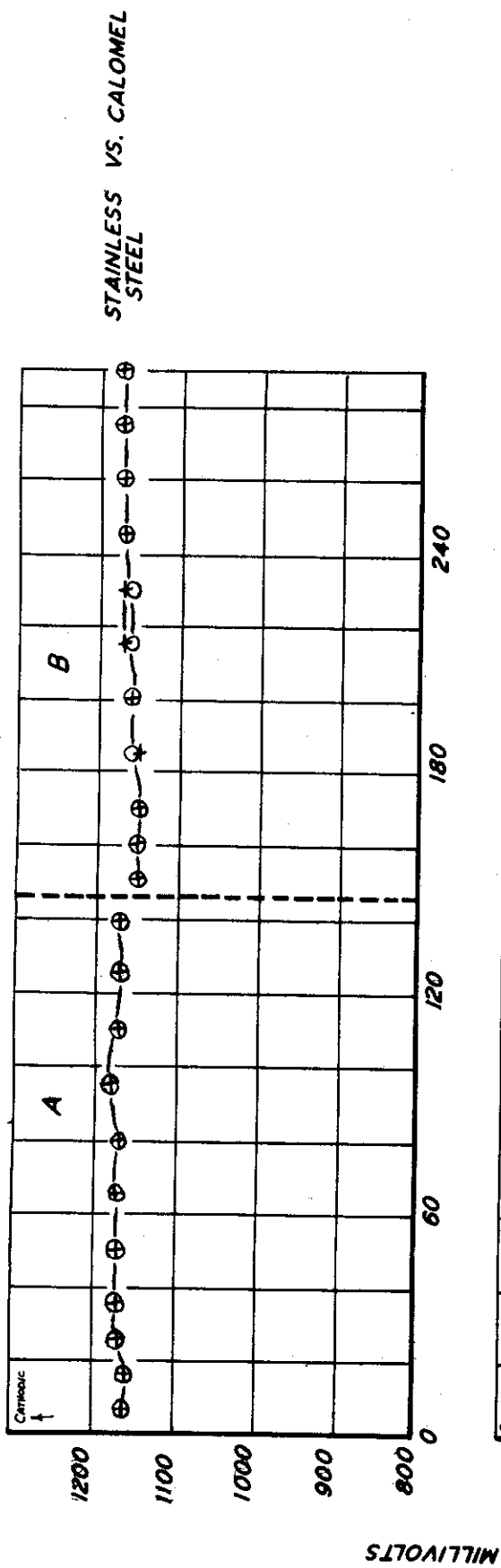
GRAPH 4   RUN 34, 55°C, 86.83% HNO_3, 12.42% NO_2, 0.75% H_2O

STAINLESS VS. CALOMEL
STEEL

ALUMINUM VS. CALOMEL

REGIONS A AND B SHOW
POTENTIAL CHANGE WITH
TIME OF 2 DIFFERENT
PAIRS OF ALUMINUM
AND STAINLESS STEEL
ELECTRODES

FIGURE 17 - EFFECT OF TIME ON POTENTIAL AT 19°C IN 12% NO₂ ACID
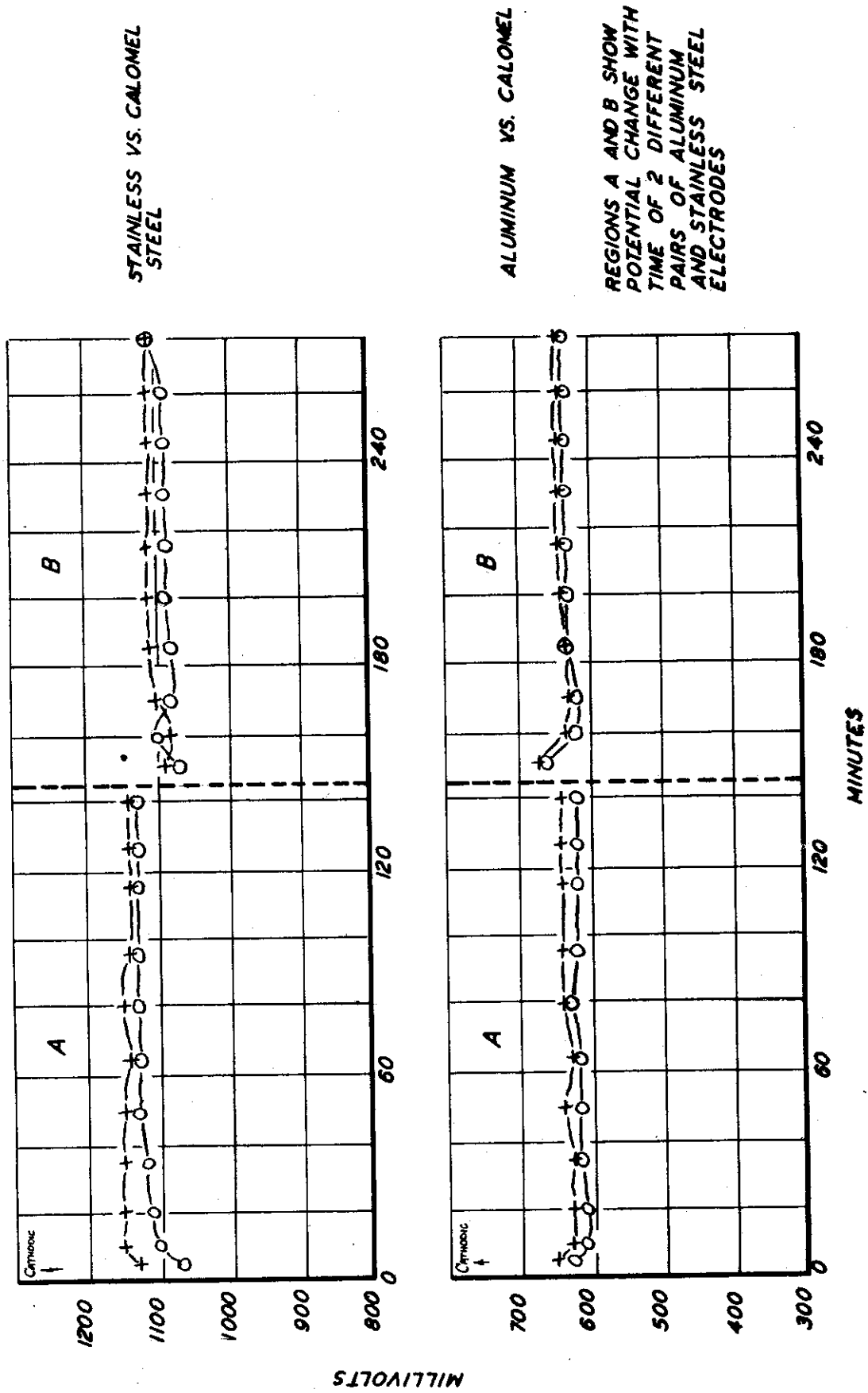
GRAPH 3   RUN 33, 19°C, 86.83% HNO₃, 12.42% NO₂, 0.75% H₂O

MILLIVOLTS
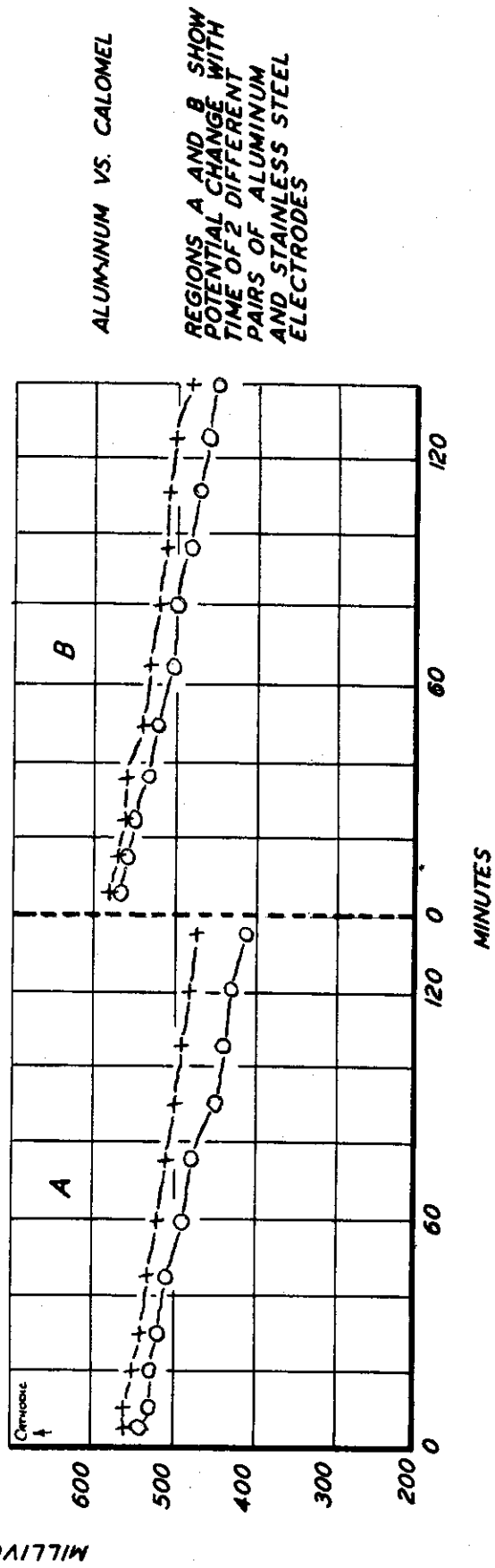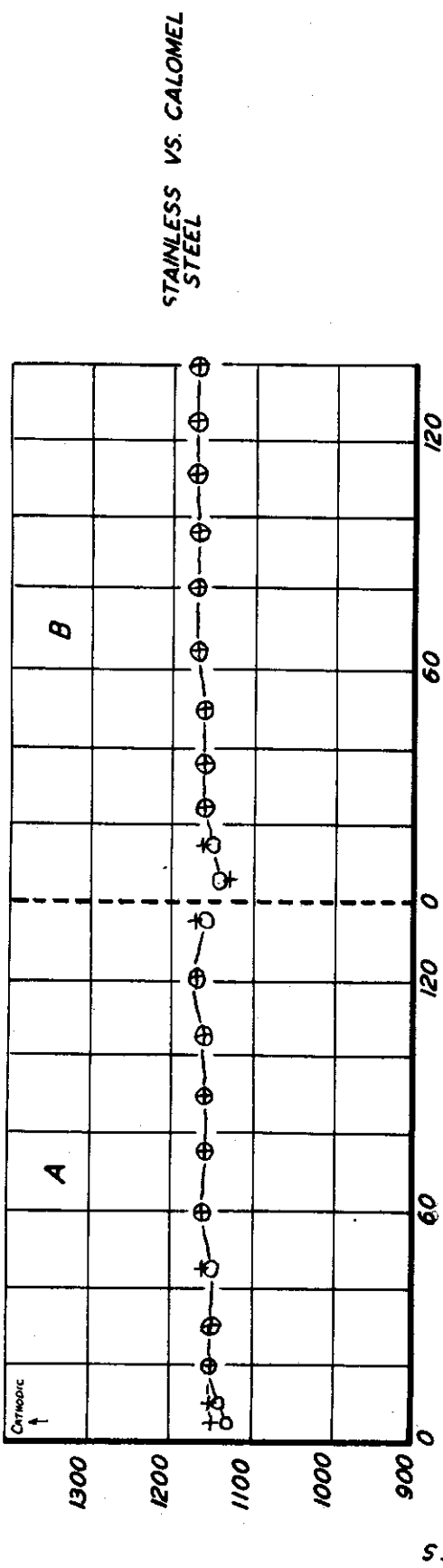
MINUTES

GRAPH 2   RUN 35, 55°C, 95.17% HNO$_3$, 4.48% NO$_2$, 0.34% H$_2$O

FIGURE 18 – EFFECT OF TIME ON POTENTIAL AT 55°C IN 14% NO$_2$ ACID

FIGURE 19 - EFFECT OF FLUORIDE ON POTENTIAL AT 19°C IN 1% NO₂ ACID
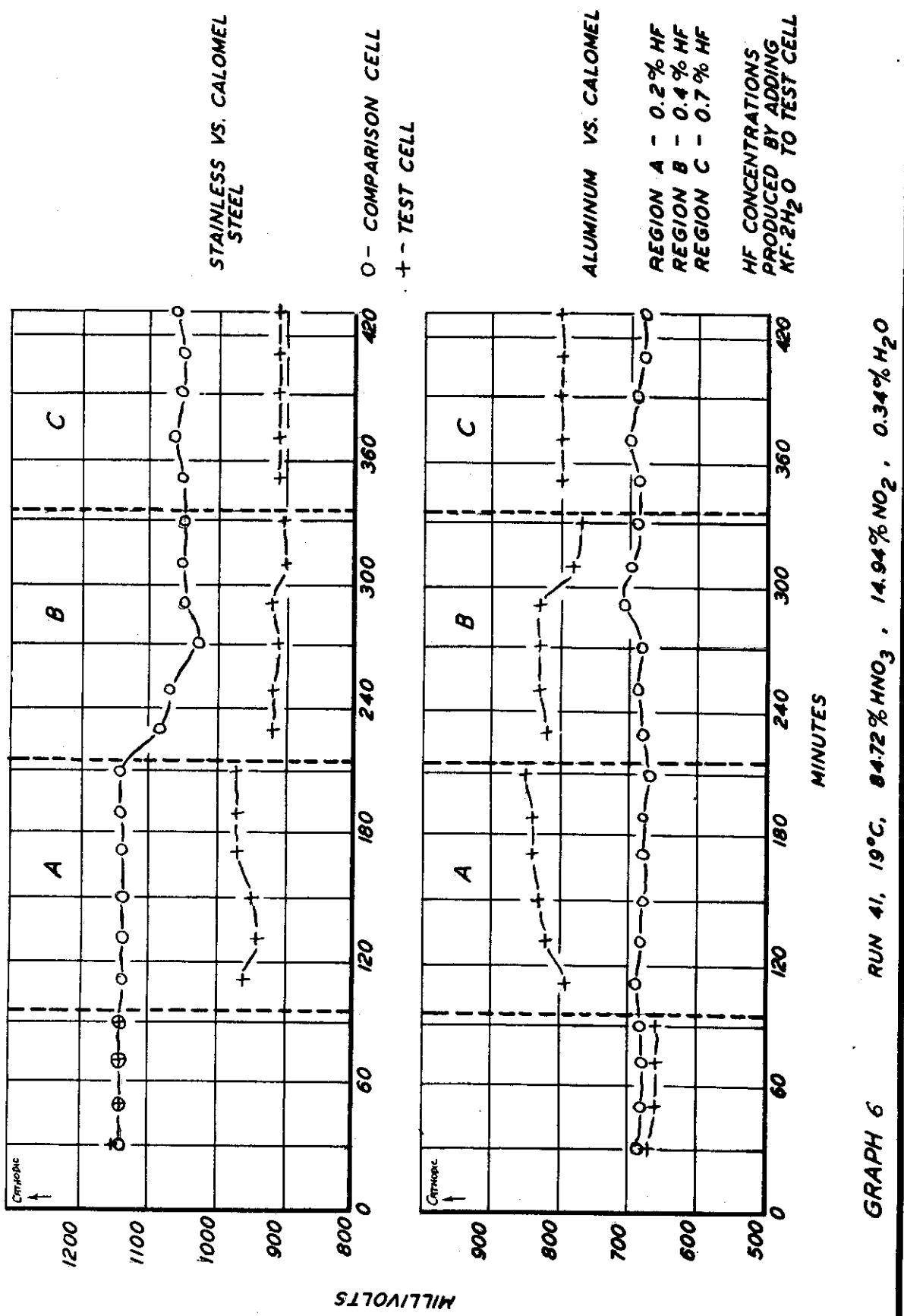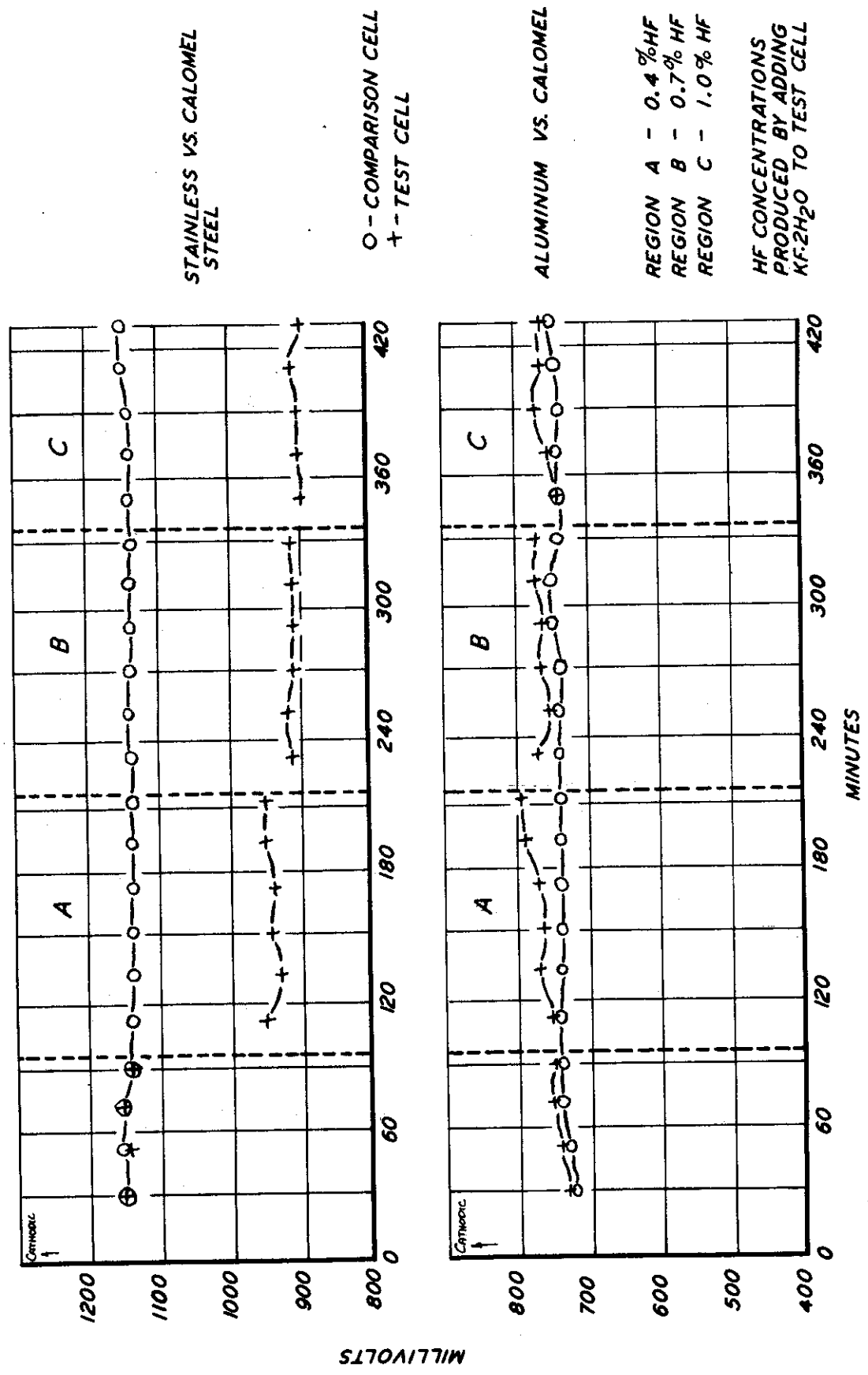
GRAPH 5   RUN 38, 19°C, 98.64% HNO₃, 0.78% NO₂, 0.59% H₂O

FIGURE 20 - EFFECT OF FLUORIDE ON POTENTIAL AT 19°C IN 15% NO₂ ACID

GRAPH 6   RUN 41, 19°C, 84.72% HNO₃, 14.94% NO₂, 0.34% H₂O

FIGURE 21 – EFFECT OF FLUORIDE ON POTENTIAL AT 19°C IN 15% NO_2 ACID

GRAPH 7   RUN 43, 19°C,   84.72 % HNO_3,   14.94 % NO_2,   0.34 % H_2O
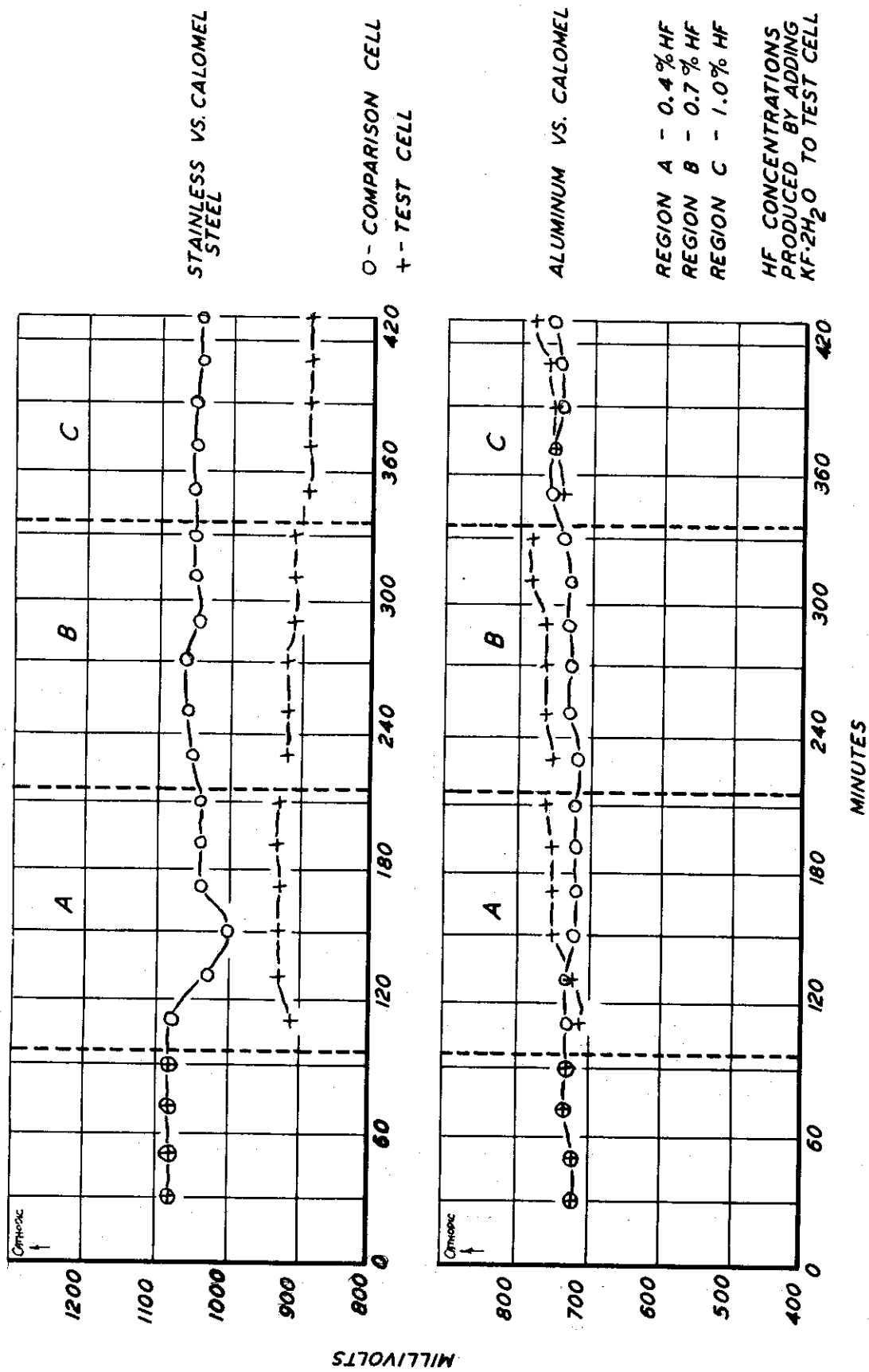
FIGURE 22 – EFFECT OF FLUORIDE ON POTENTIAL AT 17°C IN 30% NO2 ACID

RUN 44, 17°C, 69.83% HNO₃, 30.04% NO₂, 0.13% H₂O

GRAPH 8

STAINLESS VS. CALOMEL STEEL

O- COMPARISON CELL
+ - TEST CELL

ALUMINUM VS. CALOMEL

REGION A - 0.2% HF ADDED
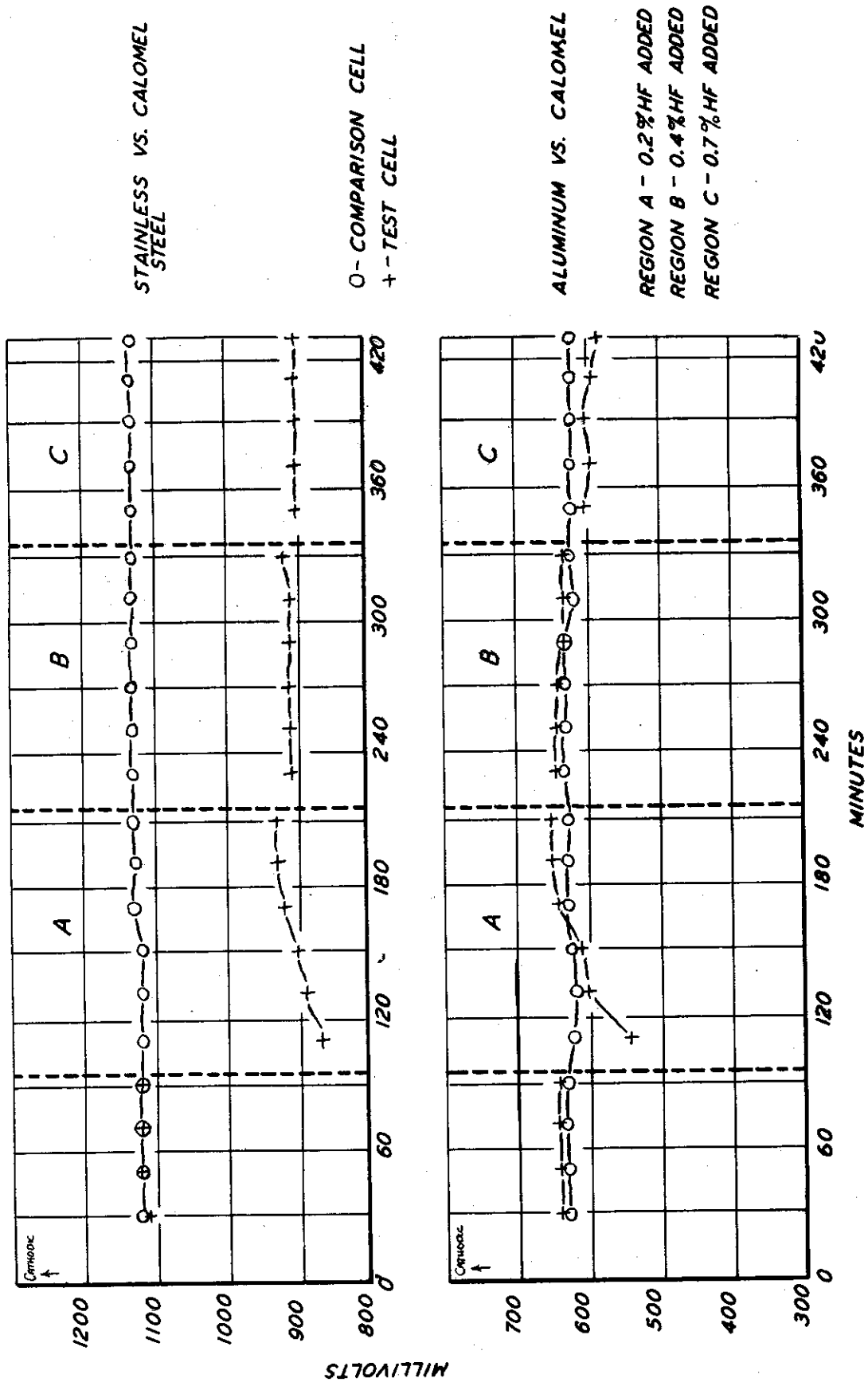REGION B - 0.4% HF ADDED
REGION C - 0.7% HF ADDED
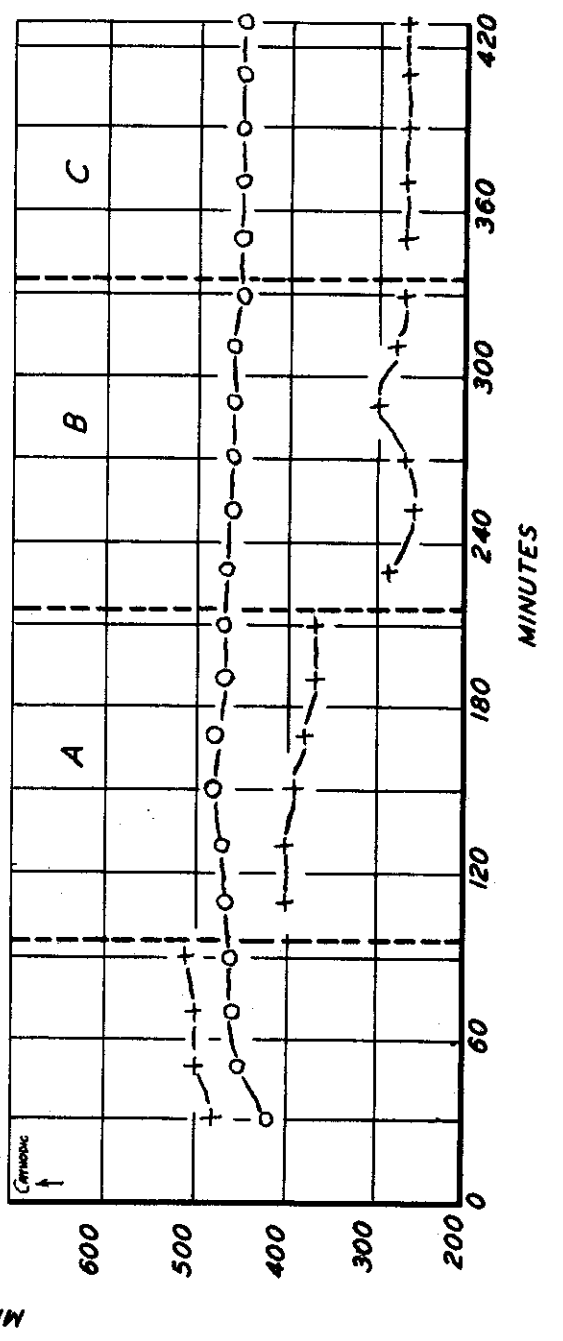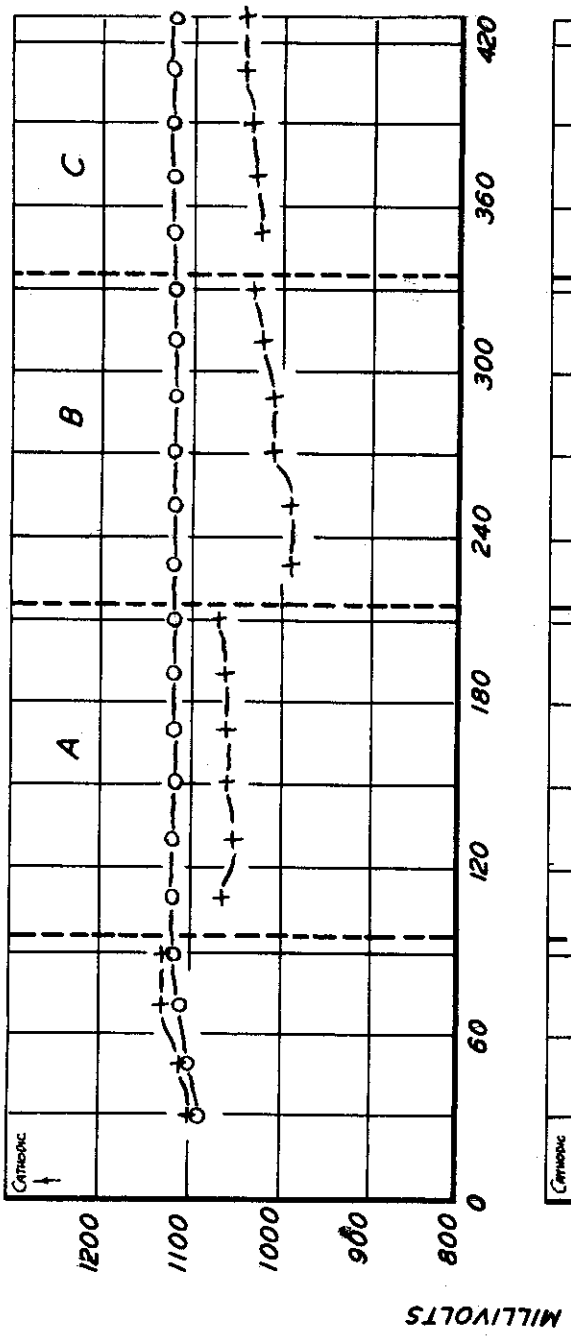
FIGURE 23 - EFFECT OF HF ON POTENTIAL AT 21°C IN 5% NO₂ ACID

GRAPH 9   RUN 46, 21°C, 92.52% HNO₃, 4.68% NO₂, 2.81% H₂O

FIGURE 24 — EFFECT OF WATER ON POTENTIAL AT 19°C IN 5% NO₂ ACID

GRAPH 10   RUN 45, 19°C, 92.52 % HNO₃, 4.68 % NO₂, 2.81 % H₂O